Aerospace Science and Technology 71 (2017) 360–372

Contents lists available at ScienceDirect

Aerospace Science and Technology

www.elsevier.com/locate/aescte

New approach to investigate nonlinear dynamic response and vibration of imperfect functionally graded carbon nanotube reinforced composite double curved shallow shells subjected to blast load and temperature

Nguyen Dinh Duc [a,b,c,*], Tran Quoc Quan [a], Nguyen Dinh Khoa [a]

[a] Advanced Materials and Structures Laboratory, VNU-Hanoi – University of Engineering and Technology (UET), 144 – Xuan Thuy – Cau Giay – Hanoi, Viet Nam
[b] National Research Laboratory, Department of Civil and Environmental Engineering, Sejong University, 209 Neungdong-ro, Gwangjin-gu, Seoul 05006, Republic of Korea
[c] Infrastructure Engineering Program, VNU-Hanoi, Vietnam Japan University (VJU), My Dinh 1 – Tu Liem – Hanoi, Viet Nam

ARTICLE INFO

Article history:
Received 24 May 2017
Received in revised form 1 September 2017
Accepted 19 September 2017
Available online 25 September 2017

Keywords:
Analytical approach
Nonlinear dynamic response and vibration
Imperfect FG-CNTRC double curved shallow shells
Blast load
Higher order shear theory
Elastic foundations

ABSTRACT

This paper presents a new approach – using analytical solution to investigate nonlinear dynamic response and vibration of imperfect functionally graded carbon nanotube reinforced composite (FG-CNTRC) double curved shallow shells. The double curved shallow shells are reinforced by single-walled carbon nanotubes (SWCNTs) which vary according to the linear functions of the shell thickness. The shells are resting on elastic foundations and subjected to blast load and temperature. The shell's effective material properties are assumed to depend on temperature and estimated through the rule of mixture. By applying higher order shear theory, Galerkin method and fourth-order Runge–Kutta method and the Airy stress function, nonlinear dynamic response and natural frequency for thick imperfect FG-CNTRC double curved shallow shells are determined. In numerical results, the influences of geometrical parameters, elastic foundations, initial imperfection, temperature increment and nanotube volume fraction on the nonlinear vibration of the FG-CNTRC double curved shallow shells are investigated. The proposed results are validated by comparing with those of other authors.

1. Introduction

Carbon nanotube-reinforced composites (CNTRCs) are an emerging class of new materials that are being developed to take advantage of the high tensile strength and electrical conductivity of carbon nanotube materials. Therefore, the problems of thermal-mechanical properties of CNTRCs have attracted increasing research effort. Zhang and Liew [1] presented post-buckling analysis of FG-CNTRC plates resting on Pasternak foundations. Shen [2] investigated thermal post-buckling analysis for nanocomposite cylindrical shells reinforced by SWCNTs subjected to a uniform temperature rise. Griebel and Hamaekers [3] examined the elastic moduli of polymer–carbon nanotube composites by molecular dynamics simulations of a SWCNT embedded in polyethylene. Kolahchi et al. [4] dealt with wave propagation of embedded viscoelastic FG-CNT-reinforced sandwich plates integrated with sensor and actuator based on refined zigzag theory. Zhang et al. [5] considered the problem of the free vibration of FG-CNT reinforced composite moderately thick rectangular plates with edges elastically restrained against transverse displacements and rotation of the plate cross section. Mirzaei and Kiani [6] studied free vibration characteristics of composite plates reinforced with single walled carbon nanotubes. The bending, vibration and buckling of embedded nano-sandwich plates based on refined zigzag theory, sinusoidal shear deformation theory, first order shear deformation theory and classical plate theory are investigated in work [7] of Kolahchi. Han and Elliott [8] analyzed molecular dynamics simulations of the elastic properties of polymer/carbon nanotube composites. Further, Song et al. [9] researched the vibration characteristics of CNT reinforced functionally graded composite cylindrical shells. Aragh et al. [10] considered natural frequencies characteristics of a continuously graded carbon nanotube-reinforced cylindrical panels based on the Eshelby–Mori–Tanaka approach. Lei et al. [11] studied buckling behavior of FG-CNTRC laminated plate using the first-order shear deformation theory. Shen and Xiang [12,13] introduced investigations on the nonlinear bending analysis and the large amplitude vibration behavior of CNTRC cylindrical panels resting on

* Corresponding author at: Advanced Materials and Structures Laboratory, VNU-Hanoi – University of Engineering and Technology (UET), 144 – Xuan Thuy – Cau Giay – Hanoi, Viet Nam.
E-mail address: ducnd@vnu.edu.vn (D.D. Nguyen).

https://doi.org/10.1016/j.ast.2017.09.031
1270-9638/

elastic foundations in thermal environments. Mirzaei et al. [14] investigated linear thermal buckling of a composite conical shell made from a polymeric matrix and reinforced with carbon nanotube fibers. Kolahchi et al. [15] investigated nonlinear dynamic stability analysis of embedded temperature-dependent viscoelastic plates reinforced by single-walled carbon nanotubes. Zhang et al. [16] presented a first known investigation on the geometrically nonlinear large deformation behavior of triangular FG-CNTRC plates under transversely distributed loads.

Noted that in all above mentioned references about FG-CNTRC plates and shells, the authors used finite element methods, analytical solution has not been yet considered.

The studies of the behaviors of composite structures under blast load have been taken much attention of researchers in the word. Zhu and Khanna [17] studied the dynamic response of a novel laminated glass panel using a transparent glass fiber-reinforced composite interlayer under blast loading. Analytical approaches to obtain maximum deformations (center) of the double skin façades panels subjected to blast pressures are presented by Ding et al. [18]. Zhang et al. [19] considered experimental investigations on the laser-welded triangular corrugated core sandwich panels and equivalent solid plates subjected to air blast loading; and Flores-Johnson et al. [20] introduced a multi-layered composite inspired by the hierarchical structure of nacre and made of layers of aluminum alloy AA 7075 bonded with toughened epoxy resin for blast resistant applications. Lam et al. [21] developed existing knowledge on the modeling of blast pressure for engineering applications. Micallef et al. [22] studied the dynamic performance of simply-supported rigid-plastic circular steel plates subjected to localized blast loading. Recently, Yao et al. [23] analyzed anti-blast performance and damage characteristics of reinforced concrete slab with different reinforcement ratios through both blast experiments and numerical simulations. Arablouei and Kodur [24] presented a fracture mechanics-based numerical approach for quantifying delamination of spray-applied fire-resistive material from a steel beam–column subjected to a blast loading. Based on Reddy's higher-order shear deformation plate theory, Duc et al. [25] investigated the nonlinear dynamic response and vibration of imperfect FGM thick plates subjected to blast and thermal loads resting on elastic foundations. Pickerd et al. [26] conducted a series of small-scale internal blast experiments to assess the structural response and failure mechanisms of metal containers subjected to internal blast loading, for the enhancement of Vulnerability/Lethality modeling. Phuong et al. [27] developed a finite element model to understand the deformation and failure mechanisms of a multi-layered elastomer/fibre-reinforced polymer composite panel under blast. Linz et al. [28] used the von Karman theory for large deflections of plates to simulate the effect of large explosions on laminated glazing.

The change of the temperature in the structural and non-structural member causes thermal stress is defined as the effect of thermal load with temperature dependent properties. In the recent years, many investigations have been carried out on the nonlinear static and dynamic responses of composite structures. Eshraghi et al. [29] introduce solution methods capable of treating static bending and free vibration problems involving thermally loaded functionally graded annular and circular micro-plates. Duc [30] presented an analytical investigation on nonlinear thermal dynamic behavior of imperfect functionally graded circular cylindrical shells eccentrically reinforced by outside stiffeners and surrounded on elastic foundations using the Reddy's third order shear deformation shell theory in thermal environment. Mirsalehi et al. [31] evaluated the buckling of a thin FGM microplate subjected to mechanical and thermal loading using the spline finite strip method, based on modified couple stress theory. Buckling behaviors of shear deformable grid-stiffened functionally graded cylindrical shells under the combined compressive and thermal loads are investigated by Sun et al. [32]. Bich et al. [33] presented an analytical approach to investigate the nonlinear dynamic response and vibration of imperfect eccentrically stiffened FGM thick double curved shallow shells on elastic foundations using both of the first order shear deformation theory. Guo et al. [34] developed an interaction energy integral method is developed for the finite element evaluation of the T-stress in non-homogeneous materials under thermal loading. Warminska et al. [35] focused on dynamics of a composite beam subjected to thermal and mechanical loadings.

Up to date, to best of the authors' knowledge, there has been recently no publication using analytical approach to investigate the static and dynamic behaviors of imperfect FG-CNTRC double curved shallow shells. A novelty of this study is that the using analytical solution and Reddy's third order shear deformation theory to study the nonlinear vibration of imperfect thick FG-CNTRC double curved shallow shells subjected to the combination of blast load and temperature. The advantage of the present analytical method is that dynamic response and frequencies are presented explicitly by the geometric parameters and material properties of the structure, as well as the extrinsic force and temperature, so we can design and modify these parameters properly to actively control the dynamic behavior of the shells. In this work, the shell's effective material properties are assumed to depend on temperature and estimated through the rule of mixture. Numerical results for dynamic response of the FG-CNTRC double curved shallow shells are obtained by Galerkin method fourth-order Runge–Kutta method.

2. Determination of the elastic modules and the thermal expansion coefficients of CNTRCs

In this study, the FG-CNTRC material is made of Poly (methyl methacrylate), referred to as PMMA, reinforced by (10, 10) SWCNTs. The effective Young's and shear modulus of the FG-CNTRC material are determined as [1,2,12–14,16]

$$\begin{aligned} E_{11} &= \eta_1 V_{CNT} E_{11}^{CNT} + V_m E_m \\ \frac{\eta_2}{E_{22}} &= \frac{V_{CNT}}{E_{22}^{CNT}} + \frac{V_m}{E_m} \\ \frac{\eta_3}{G_{12}} &= \frac{V_{CNT}}{G_{12}^{CNT}} + \frac{V_m}{G_m} \end{aligned} \tag{1}$$

where $E_{11}^{CNT}, E_{11}^{CNT}, G_{12}^{CNT}$ are Young's and shear modulus of the CNT; E_m, G_m are mechanical properties of the matrix. V_{CNT} and V_m are the volume fractions of the CNT and the matrix, respectively and η_i $(i = \overline{1,3})$ are the CNT efficiency parameters.

The volume fractions of the CNT and the matrix are assumed to change according to the linear functions of the shell thickness. Three types of FG-CNTRCs, i.e. FG-V, FG-O and FG-X, are considered. Specifically, the volume fractions of the three distribution types are expressed as follows [6,14,16]

$$\begin{aligned} V_{CNT}(z) &= \begin{cases} 2V_{VCT}^*(1 - 2\frac{|z|}{h}) & \text{(FG-O)} \\ 4V_{VCT}^*\frac{|z|}{h} & \text{(FG-X)} \\ V_{VCT}^*(1 + 2\frac{z}{h}) & \text{(FG-V)} \end{cases} \\ V_m(z) &= 1 - V_{CNT}(z) \end{aligned} \tag{2}$$

where

$$V_{CNT}^* = \frac{w_{CNT}}{w_{CNT} + (\rho_{CNT}/\rho_m) - (\rho_{CNT}/\rho_m) w_{CNT}} \tag{3}$$

in which w_{CNT} is the mass fraction of CNTs, and ρ_{CNT} and ρ_m are the densities of CNT and matrix, respectively.

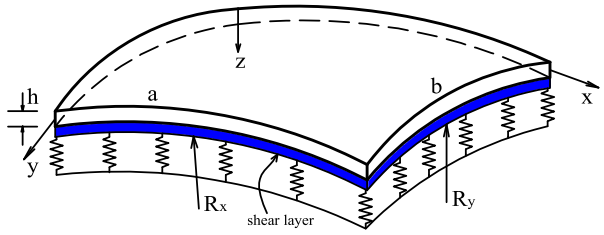

Fig. 1. Geometry and coordinate system of FG-CNTRC double curved shallow shells on elastic foundations.

Except Poisson's ratio, the material properties of the matrix are assumed to express as linear functions of temperature [1,2,12–14,16]

$$\begin{aligned}&\nu_m = 0.34\\&\alpha_m = 45(1+0.0005\Delta T)\times 10^{-6}/\mathrm{K}\\&E_m = (3.52-0.0034T)\ \mathrm{GPa}\end{aligned} \tag{4}$$

with $T = T_0 + \Delta T$, ΔT is the temperature increment in the environment containing the material and $T_0 = 300$ K (room temperature).

For the CNT, the material properties of $(10, 10)$ SWCNTs are highly dependent to temperature. Shen and Xiang [12] reported these properties at five certain temperature levels, i.e. $T = 300$ K, 400 K, 500 K, 700 K, 1000 K. Specifically, Young's modulus, shear modulus and thermal expansion coefficient of SWCNTs are listed in Table 1. The Poisson's ratio of SWCNTs is chosen to be constant $\nu_{12}^{CNT} = 0.175$.

The CNT efficiency parameters η_i $(i = \overline{1,3})$ used in Eq. (1) are estimated by matching Young's modulus E_{11} and E_{22} and the shear modulus G_{12} of FG-CNTRC material obtained by the extended rule of mixture to molecular simulation results [1,2,12–14,16]. For three different volume fraction of CNTs, these parameters are as: $\eta_1 = 0.137, \eta_2 = 1.022, \eta_3 = 0.715$ for the case of $V_{CNT}^* = 0.12$ (12%); $\eta_1 = 0.142, \eta_2 = 1.626, \eta_3 = 1.138$ for the case of $V_{CNT}^* = 0.17$ (17%) and $\eta_1 = 0.141, \eta_2 = 1.585, \eta_3 = 1.109$ for the case of $V_{CNT}^* = 0.28$ (28%).

The effective Poisson's ratio depends weakly on temperature change and position and is given as [1,2,12–14,16]

$$\nu_{12} = V_{CNT}^* \nu_{12}^{CNT} + V_m \nu_m \tag{5}$$

where ν_{12}^{CNT} and ν_m are Poisson's ratio of the CNT and the matrix, respectively.

The thermal expansion coefficients in the longitudinal and transverse directions of the CNTRCs are expressed by [1,2,12–14,16]

$$\begin{aligned}&\alpha_{11} = \frac{V_{CNT}E_{11}^{CNT}\alpha_{11}^{CNT} + V_m E_m \alpha_m}{V_{CNT}E_{11}^{CNT} + V_m E_m}\\&\alpha_{22} = \left(1+\nu_{12}^{CNT}\right)V_{CNT}\alpha_{22}^{CNT} + (1+\nu_m)V_m\alpha_m - \nu_{12}\alpha_{11}\end{aligned} \tag{6}$$

with $\alpha_{11}^{CNT}, \alpha_{22}^{CNT}$ and α_m are the thermal expansion coefficients of the CNT and the matrix, respectively.

3. Theoretical formulation

Consider a FG-CNTRC double curved shallow shell of radii of curvature R_x, R_y, length of edges a, $A_2 = \frac{E_1\lambda_m^2}{32\delta_n^2}W(W+2\mu h)$ and uniform thickness h resting on elastic foundations in thermal environments. A coordinate system (x, y, z) is established in which (x, y) plane on the middle surface of the shell and z on thickness direction $(-h/2 \le z \le h/2)$ as shown in Fig. 1.

In this study, third order shear theory is used to derive basic equations to investigate the nonlinear vibration of thick FG-CNTRC double curved shallow shells on elastic foundations subjected to blast and thermal loads.

The geometrical compatibility equation for an imperfect FG-CNTRC double curved shallow shell is defined as [39–42]

$$\begin{aligned}&\frac{\partial^2\varepsilon_x^0}{\partial y^2} + \frac{\partial^2\varepsilon_y^0}{\partial x^2} - \frac{\partial^2\gamma_{xy}^0}{\partial x\partial y}\\&\quad= \frac{\partial^2 w^2}{\partial x\partial y} - \frac{\partial^2 w}{\partial x^2}\frac{\partial^2 w}{\partial y^2} + 2\frac{\partial^2 w}{\partial x\partial y}\frac{\partial^2 w^*}{\partial x\partial y} - \frac{\partial^2 w}{\partial x^2}\frac{\partial^2 w^*}{\partial y^2}\\&\qquad - \frac{\partial^2 w}{\partial y^2}\frac{\partial^2 w^*}{\partial x^2} - \frac{1}{R_x}\frac{\partial^2 w}{\partial y^2} - \frac{1}{R_y}\frac{\partial^2 w}{\partial x^2}\end{aligned} \tag{7}$$

in which imperfection function $w^*(x, y)$ denotes initial small imperfection of FG-CNTRC shell.

The nonlinear equilibrium equation of thick FG-CNTRC double curved shallow shells are written as [39–42]

$$\frac{\partial N_x}{\partial x} + \frac{\partial N_{xy}}{\partial y} = \overline{I}_1\frac{\partial^2 u}{\partial t^2} + \overline{I}_2\frac{\partial^2\phi_x}{\partial t^2} - \overline{I}_3\frac{\partial^3 w}{\partial t^2\partial x} \tag{8a}$$

$$\frac{\partial N_{xy}}{\partial x} + \frac{\partial N_y}{\partial y} = \overline{I}_1^*\frac{\partial^2 v}{\partial t^2} + \overline{I}_2^*\frac{\partial^2\phi_y}{\partial t^2} - \overline{I}_3^*\frac{\partial^3 w}{\partial t^2\partial y} \tag{8b}$$

$$\begin{aligned}&\frac{\partial Q_x}{\partial x} + \frac{\partial Q_y}{\partial y} - 3c_1\left(\frac{\partial R_x}{\partial x} + \frac{\partial R_y}{\partial y}\right)\\&\quad + c_1\left(\frac{\partial^2 P_x}{\partial x^2} + 2\frac{\partial^2 P_y}{\partial x\partial y} + \frac{\partial^2 P_y}{\partial y^2}\right) + \frac{N_x}{R_x} + \frac{N_y}{R_y} + q + N_x\frac{\partial^2 w}{\partial x^2}\\&\quad + 2N_{xy}\frac{\partial^2 w}{\partial x\partial y} + N_y\frac{\partial^2 w}{\partial y^2} - k_1 w + k_2\nabla^2 w\\&= I_1\frac{\partial^2 w}{\partial t^2} + 2\varepsilon I_1\frac{\partial w}{\partial t} + \overline{I}_3\frac{\partial^3 u}{\partial t^2\partial x} + \overline{I}_5\frac{\partial^3\phi_x}{\partial t^2\partial x}\\&\quad + \overline{I}_3^*\frac{\partial^3 v}{\partial t^2\partial y} + \overline{I}_5^*\frac{\partial^3\phi_y}{\partial t^2\partial y} - c_1^2 I_7\left(\frac{\partial^4 w}{\partial t^2\partial x^2} + \frac{\partial^4 w}{\partial t^2\partial y^2}\right)\end{aligned} \tag{8c}$$

$$\begin{aligned}&\frac{\partial M_x}{\partial x} + \frac{\partial M_{xy}}{\partial y} - Q_x + 3c_1R_x - c_1\left(\frac{\partial P_x}{\partial x} + \frac{\partial P_{xy}}{\partial y}\right)\\&\quad= \overline{I}_2\frac{\partial^2 u}{\partial t^2} + \overline{I}_4\frac{\partial^2\phi_x}{\partial t^2} - \overline{I}_5\frac{\partial^3 w}{\partial t^2\partial x}\end{aligned} \tag{8d}$$

$$\begin{aligned}&\frac{\partial M_{xy}}{\partial x} + \frac{\partial M_y}{\partial y} - Q_y + 3c_1R_y - c_1\left(\frac{\partial P_{xy}}{\partial x} + \frac{\partial P_y}{\partial y}\right)\\&\quad= \overline{I}_2^*\frac{\partial^2 v}{\partial t^2} + \overline{I}_4^*\frac{\partial^2\phi_y}{\partial t^2} - \overline{I}_5^*\frac{\partial^3 w}{\partial t^2\partial y}\end{aligned} \tag{8e}$$

in which u, v, w are displacement components corresponding to the coordinates (x, y, z), ϕ_x, ϕ_y are the slopes of the transverse normal about the x and y axes at $z = 0$, respectively, k_1 is Winkler foundation modulus, k_2 is the shear layer foundation stiffness of Pasternak model, ε is the viscous damping coefficient and

$$\begin{aligned}&\overline{I}_1 = I_1 + \frac{2I_2}{R_x}, \qquad \overline{I}_1^* = I_1 + \frac{2I_2}{R_y},\\&\overline{I}_2 = I_2 + \frac{I_3}{R_x} - c_1I_4 - \frac{c_1I_5}{R_x}, \qquad \overline{I}_2^* = I_2 + \frac{I_3}{R_y} - c_1I_4 - \frac{c_1I_5}{R_y}\\&\overline{I}_3 = c_1I_4 + \frac{c_1I_5}{R_x}, \qquad \overline{I}_3^* = c_1I_4 + \frac{c_1I_5}{R_y},\\&\overline{I}_4 = \overline{I}_4^* = I_3 - 2c_1I_5 + c_1^2I_7, \qquad \overline{I}_5 = \overline{I}_5^* = c_1I_5 - c_1^2I_7\\&(I_1, I_2, I_3, I_4, I_5, I_7) = \int_{-h/2}^{h/2}\rho(z)\left(1, z, z^2, z^3, z^4, z^6\right)dz\\&\rho(z) = V_{CNT}\rho_{CNT} + V_m\rho_m\end{aligned} \tag{9}$$

Table 1
Temperature-dependent material properties for (10, 10) SWCNTs [12].

T (K)	E_{11}^{CNT} (TPa)	E_{22}^{CNT} (TPa)	G_{12}^{CNT} (TPa)	α_{11}^{CNT} ($\times 10^{-6}$/K)	α_{22}^{CNT} ($\times 10^{-6}$/K)
300	5.6466	7.0800	1.9445	3.4584	5.1682
400	5.5679	6.9814	1.9703	4.1496	5.0905
500	5.5308	6.9348	1.9643	4.5361	5.0189
700	5.4744	6.8641	1.9644	4.6677	4.8943
1000	5.2814	6.6220	1.9451	4.2800	4.7532

The blast load $q(t)$ is a short-term load and is generated by an explosion or by a shock–wave disturbance produced by an aircraft flying at supersonic speed, or by a supersonic projectile, rocket or missile operating in its vicinity. It can be written as [21]

$$q(t) = 1.8\ Ps_{max}\left(1 - \frac{t}{T_s}\right)\exp\left(\frac{-bt}{T_s}\right) \tag{10}$$

where the "1.8" factor accounts for the effects of a hemispherical blast, Ps_{max} is the maximum (or peak) static over-pressure, b is the parameter controlling the rate of wave amplitude decay and T_s is the parameter characterizing the duration of the blast pulse.

The normal strains in the middle surface of FG-CNTRC double curved shallow shells may be expressed by

$$\begin{bmatrix}\varepsilon_x^0\\ \varepsilon_y^0\\ \gamma_{xy}^0\end{bmatrix} = \begin{bmatrix}\frac{\partial u}{\partial x} - \frac{w}{R_x} + \frac{1}{2}(\frac{\partial w}{\partial x})^2\\ \frac{\partial v}{\partial y} - \frac{w}{R_y} + \frac{1}{2}(\frac{\partial w}{\partial y})^2\\ \frac{\partial u}{\partial y} + \frac{\partial v}{\partial x} + \frac{\partial w}{\partial x}\frac{\partial w}{\partial y}\end{bmatrix},$$
$$\begin{bmatrix}\gamma_{xz}^0\\ \gamma_{yz}^0\end{bmatrix} = -3c_1\begin{bmatrix}\frac{\partial w}{\partial x} + \phi_x\\ \frac{\partial w}{\partial y} + \phi_y\end{bmatrix} \tag{11}$$

Based on third order shear theory, the strain-displacement relations taking into account von Karman nonlinear terms and are [42–44]

$$\begin{bmatrix}\varepsilon_x\\ \varepsilon_y\\ \gamma_{xy}\end{bmatrix} = \begin{bmatrix}\varepsilon_x^0\\ \varepsilon_y^0\\ \gamma_{xy}^0\end{bmatrix} + z\begin{bmatrix}k_x^1\\ k_y^1\\ k_{xy}^1\end{bmatrix} + z^3\begin{bmatrix}k_x^3\\ k_y^3\\ k_{xy}^3\end{bmatrix},$$
$$\begin{bmatrix}\gamma_{xz}\\ \gamma_{yz}\end{bmatrix} = \begin{bmatrix}\gamma_{xz}^0\\ \gamma_{yz}^0\end{bmatrix} + z^2\begin{bmatrix}k_{xz}^2\\ k_{yz}^2\end{bmatrix} \tag{12}$$

with

$$\begin{bmatrix}k_x^1\\ k_y^1\\ k_{xy}^1\end{bmatrix} = \begin{bmatrix}\frac{\partial \phi_x}{\partial x}\\ \frac{\partial \phi_y}{\partial y}\\ \frac{\partial \phi_x}{\partial y} + \frac{\partial \phi_y}{\partial y}\end{bmatrix},$$
$$\begin{bmatrix}k_x^3\\ k_y^3\\ k_{xy}^3\end{bmatrix} = -c_1\begin{bmatrix}\frac{\partial \phi_x}{\partial x} + \frac{\partial^2 w}{\partial x^2}\\ \frac{\partial \phi_y}{\partial y} + \frac{\partial^2 w}{\partial y^2}\\ \frac{\partial \phi_x}{\partial y} + \frac{\partial \phi_y}{\partial y} + 2\frac{\partial^2 w}{\partial x \partial y}\end{bmatrix},$$
$$\begin{bmatrix}k_{xz}^2\\ k_{yz}^2\end{bmatrix} = -3c_1\begin{bmatrix}\frac{\partial w}{\partial x} + \phi_x\\ \frac{\partial w}{\partial y} + \phi_y\end{bmatrix} \tag{13}$$

Hooke's law for a FG-CNTRC double curved shallow shell with temperature-dependent properties is defined as [11]

$$\begin{bmatrix}\sigma_{xx}\\ \sigma_{yy}\\ \sigma_{xy}\\ \sigma_{xz}\\ \sigma_{yz}\end{bmatrix} = \begin{bmatrix}Q_{11} & Q_{12} & 0 & 0 & 0\\ Q_{12} & Q_{22} & 0 & 0 & 0\\ 0 & 0 & Q_{66} & 0 & 0\\ 0 & 0 & 0 & Q_{44} & 0\\ 0 & 0 & 0 & 0 & Q_{55}\end{bmatrix}\begin{bmatrix}\varepsilon_{xx} - \alpha_{11}\Delta T\\ \varepsilon_{yy} - \alpha_{22}\Delta T\\ \varepsilon_{xy}\\ \varepsilon_{xz}\\ \varepsilon_{yz}\end{bmatrix} \tag{14}$$

where

$$Q_{11} = \frac{E_{11}}{1 - \nu_{12}\nu_{21}}, \qquad Q_{22} = \frac{E_{22}}{1 - \nu_{12}\nu_{21}},$$
$$Q_{12} = \frac{\nu_{21}E_{11}}{1 - \nu_{12}\nu_{21}}, \qquad Q_{44} = G_{23}, \tag{15}$$
$$Q_{55} = G_{13}, \qquad Q_{44} = G_{12}$$

and we assume that $G_{13} = G_{12}$ and $G_{23} = 1.2G_{12}$ [2].

The force and moment resultants of FG-CNTRC double curved shallow shells are given by

$$(N_i, M_i, P_i) = \int_{-h/2}^{h/2}\sigma_i\left(1, z, z^3\right)dz, \quad i = x, y, xy$$
$$(Q_i, K_i) = \int_{-h/2}^{h/2}\sigma_{iz}\left(1, z^2\right)dz, \quad i = x, y \tag{16}$$

Substitution of Eqs. (12) into Eqs. (14) and the result into Eqs. (16) yields the constitutive relations as

$$\begin{aligned}
N_x &= A_{11}\varepsilon_x^0 + A_{12}\varepsilon_y^0 + B_{11}k_x^1 + B_{12}k_y^1 + E_{11}k_x^3 + E_{12}k_y^3 - \Phi_1\\
N_y &= A_{12}\varepsilon_x^0 + A_{22}\varepsilon_y^0 + B_{12}k_x^1 + B_{22}k_y^1 + E_{12}k_x^3 + E_{22}k_y^3 - \Phi_2\\
N_{xy} &= A_{66}\gamma_{xy}^0 + B_{66}k_{xy}^1 + E_{66}k_{xy}^3\\
M_x &= B_{11}\varepsilon_x^0 + B_{12}\varepsilon_y^0 + D_{11}k_x^1 + D_{12}k_y^1 + F_{11}k_x^3 + F_{12}k_y^3 - \Phi_3\\
M_y &= B_{12}\varepsilon_x^0 + B_{22}\varepsilon_y^0 + D_{12}k_x^1 + D_{22}k_y^1 + F_{12}k_x^3 + F_{22}k_y^3 - \Phi_4\\
M_{xy} &= B_{66}\gamma_{xy}^0 + D_{66}k_{xy}^1 + F_{66}k_{xy}^3\\
P_x &= E_{11}\varepsilon_x^0 + E_{12}\varepsilon_y^0 + F_{11}k_x^1 + F_{12}k_y^1 + H_{11}k_x^3 + H_{12}k_y^3 - \Phi_5\\
P_y &= E_{12}\varepsilon_x^0 + E_{22}\varepsilon_y^0 + F_{12}k_x^1 + F_{22}k_y^1 + H_{12}k_x^3 + H_{22}k_y^3 - \Phi_6\\
P_{xy} &= E_{66}\gamma_{xy}^0 + F_{66}k_{xy}^1 + H_{66}k_{xy}^3\\
Q_x &= A_{44}\gamma_{xz}^0 + D_{44}k_{xz}^2, \qquad Q_y = A_{55}\gamma_{yz}^0 + D_{55}k_{yz}^2\\
K_x &= D_{44}\gamma_{xz}^0 + F_{44}k_{xz}^2, \qquad K_y = D_{55}\gamma_{yz}^0 + F_{55}k_{yz}^2
\end{aligned} \tag{17}$$

in which

$$(A_{ij}, B_{ij}, D_{ij}, E_{ij}, F_{ij}, H_{ij}) = \int_{-h/2}^{h/2} Q_{ij}\left(1, z, z^2, z^3, z^4, z^6\right)dz,$$

$$ij = 11, 12, 22, 66$$

$$(A_{kl}, D_{kl}, F_{kl}) = \int_{-h/2}^{h/2} Q_{ij}\left(1, z^2, z^4\right)dz, \quad kl = 44, 55$$

$$\begin{aligned}
\Phi_1 &= \int_{-h/2}^{h/2} Q_{11}\alpha_{11}\Delta T dz + \int_{-h/2}^{h/2} Q_{12}\alpha_{22}\Delta T dz,\\
\Phi_2 &= \int_{-h/2}^{h/2} Q_{12}\alpha_{11}\Delta T dz + \int_{-h/2}^{h/2} Q_{22}\alpha_{22}\Delta T dz\\
\Phi_3 &= \int_{-h/2}^{h/2} Q_{11}\alpha_{11}\Delta T z dz + \int_{-h/2}^{h/2} Q_{12}\alpha_{22}\Delta T z dz,\\
\Phi_4 &= \int_{-h/2}^{h/2} Q_{12}\alpha_{11}\Delta T z dz + \int_{-h/2}^{h/2} Q_{22}\alpha_{22}\Delta T z dz\\
\Phi_5 &= \int_{-h/2}^{h/2} Q_{11}\alpha_{11}\Delta T z^3 dz + \int_{-h/2}^{h/2} Q_{12}\alpha_{22}\Delta T z^3 dz,\\
\Phi_6 &= \int_{-h/2}^{h/2} Q_{12}\alpha_{11} z^3\Delta T dz + \int_{-h/2}^{h/2} Q_{22}\alpha_{22} z^3\Delta T dz
\end{aligned} \tag{18}$$

From the constitutive relations (13) and (17), one can write

$$\begin{aligned}
\varepsilon_x^0 &= I_{11}\frac{\partial^2 f}{\partial y^2} - I_{12}\frac{\partial^2 f}{\partial x^2} + I_{13}\frac{\partial \phi_x}{\partial x} + I_{14}\frac{\partial \phi_y}{\partial y}\\
&\quad - c_1 I_{15}\left(\frac{\partial^2 w}{\partial x^2} + \frac{\partial \phi_x}{\partial x}\right)\\
&\quad - c_1 I_{16}\left(\frac{\partial^2 w}{\partial y^2} + \frac{\partial \phi_y}{\partial y}\right) + I_{17}\Phi_1 + I_{18}\Phi_2\\
\varepsilon_y^0 &= I_{21}\frac{\partial^2 f}{\partial x^2} - I_{12}\frac{\partial^2 f}{\partial y^2} + I_{23}\frac{\partial \phi_x}{\partial x} + I_{24}\frac{\partial \phi_y}{\partial y}\\
&\quad - c_1 I_{25}\left(\frac{\partial^2 w}{\partial x^2} + \frac{\partial \phi_x}{\partial x}\right)\\
&\quad - c_1 I_{26}\left(\frac{\partial^2 w}{\partial y^2} + \frac{\partial \phi_y}{\partial y}\right) + I_{27}\Phi_1 + I_{28}\Phi_2\\
\gamma_{xy}^0 &= -I_{31}\frac{\partial^2 f}{\partial x \partial y} + I_{32}\left(\frac{\partial \phi_x}{\partial y} + \frac{\partial \phi_y}{\partial x}\right)\\
&\quad - c_1 I_{33}\left(2\frac{\partial^2 w}{\partial x \partial y} + \frac{\partial \phi_x}{\partial y} + \frac{\partial \phi_y}{\partial x}\right)
\end{aligned} \tag{19}$$

with

$$\begin{aligned}
&\Delta = A_{11}A_{22} - A_{12}^2, \qquad I_{11} = \frac{A_{22}}{\Delta}, \qquad I_{12} = \frac{A_{12}}{\Delta},\\
&I_{13} = \frac{B_{12}A_{12} - B_{11}A_{22}}{\Delta}, \qquad I_{14} = \frac{B_{22}A_{12} - B_{12}A_{22}}{\Delta}\\
&I_{15} = \frac{E_{12}A_{12} - E_{11}A_{22}}{\Delta}, \qquad I_{16} = \frac{E_{22}A_{12} - E_{12}A_{22}}{\Delta},\\
&I_{17} = \frac{A_{22}}{\Delta}, \qquad I_{18} = -\frac{A_{12}}{\Delta}
\end{aligned}$$

$$\begin{aligned}
&I_{21} = \frac{A_{11}}{\Delta}, \qquad I_{23} = \frac{B_{11}A_{12} - B_{12}A_{11}}{\Delta},\\
&I_{24} = \frac{B_{12}A_{12} - B_{22}A_{11}}{\Delta}, \qquad I_{25} = \frac{E_{11}A_{12} - E_{12}A_{11}}{\Delta}\\
&I_{26} = \frac{E_{12}A_{12} - E_{22}A_{11}}{\Delta}, \qquad I_{27} = -\frac{A_{12}}{\Delta}, \qquad I_{28} = \frac{A_{11}}{\Delta},\\
&I_{31} = \frac{1}{A_{66}}, \qquad I_{32} = -\frac{B_{66}}{A_{66}}, \qquad I_{33} = -\frac{E_{66}}{A_{66}}
\end{aligned} \tag{20}$$

and the Airy's stress function $f(x, y, t)$ is defined as [42,44]:

$$N_x = \frac{\partial^2 f}{\partial y^2}, \qquad N_y = \frac{\partial^2 f}{\partial x^2}, \qquad N_{xy} = -\frac{\partial^2 f}{\partial x \partial y} \tag{21}$$

Imposing Eq. (21) into Eqs. (8a) and (8b) yields

$$\frac{\partial^2 u}{\partial t^2} = -\frac{\overline{I}_2}{\overline{I}_1}\frac{\partial^2 \phi_x}{\partial t^2} + \frac{\overline{I}_3}{\overline{I}_1}\frac{\partial^3 w}{\partial t^2 \partial x} \tag{22a}$$

$$\frac{\partial^2 v}{\partial t^2} = -\frac{\overline{I}_2^*}{\overline{I}_1^*}\frac{\partial^2 \phi_y}{\partial t^2} + \frac{\overline{I}_3^*}{\overline{I}_1^*}\frac{\partial^3 w}{\partial t^2 \partial y} \tag{22b}$$

By substituting Eqs. (22a) and (22b) into Eqs. (8c)–(8e) leads to

$$\begin{aligned}
&\frac{\partial Q_x}{\partial x} + \frac{\partial Q_y}{\partial y} - 3c_1\left(\frac{\partial K_x}{\partial x} + \frac{\partial K_y}{\partial y}\right)\\
&\quad + c_1\left(\frac{\partial^2 P_x}{\partial x^2} + 2\frac{\partial^2 P_y}{\partial x \partial y} + \frac{\partial^2 P_y}{\partial y^2}\right) + \frac{\partial^2 f}{\partial y^2}\frac{\partial^2 w}{\partial x^2}\\
&\quad - 2\frac{\partial^2 f}{\partial x \partial y}\frac{\partial^2 w}{\partial y^2} + \frac{\partial^2 f}{\partial x^2}\frac{\partial^2 w}{\partial y^2} + q - k_1 w + k_2\nabla^2 w\\
&\quad + \frac{1}{R_x}\frac{\partial^2 f}{\partial x^2} + \frac{1}{R_y}\frac{\partial^2 f}{\partial y^2}\\
&= I_1\frac{\partial^2 w}{\partial t^2} + 2\varepsilon I_1\frac{\partial w}{\partial t} + \overline{\overline{I}}_5\frac{\partial^3 \phi_x}{\partial t^2 \partial x} + \overline{\overline{I}}_5^*\frac{\partial^3 \phi_y}{\partial t^2 \partial y}\\
&\quad + \overline{\overline{I}}_7\frac{\partial^4 w}{\partial t^2 \partial x^2} + \overline{\overline{I}}_7^*\frac{\partial^4 w}{\partial t^2 \partial y^2}
\end{aligned} \tag{23a}$$

$$\begin{aligned}
&\frac{\partial M_x}{\partial x} + \frac{\partial M_{xy}}{\partial y} - Q_x + 3c_1 K_x - c_1\left(\frac{\partial P_x}{\partial x} + \frac{\partial P_{xy}}{\partial y}\right)\\
&= \overline{\overline{I}}_3\frac{\partial^2 \phi_x}{\partial t^2} - \overline{\overline{I}}_5\frac{\partial^3 w}{\partial t^2 \partial x}
\end{aligned} \tag{23b}$$

$$\begin{aligned}
&\frac{\partial M_{xy}}{\partial x} + \frac{\partial M_y}{\partial y} - Q_y + 3c_1 K_y - c_1\left(\frac{\partial P_{xy}}{\partial x} + \frac{\partial P_y}{\partial y}\right)\\
&= \overline{\overline{I}}_3^*\frac{\partial^2 \phi_y}{\partial t^2} - \overline{\overline{I}}_5^*\frac{\partial^3 w}{\partial t^2 \partial y}
\end{aligned} \tag{23c}$$

in which

$$\begin{aligned}
&\overline{\overline{I}}_3 = \overline{I}_4 - (\overline{I}_2)^2/\overline{I}_1, \qquad \overline{\overline{I}}_3^* = \overline{I}_4^* - (\overline{I}_2^*)^2/\overline{I}_1^*,\\
&\overline{\overline{I}}_3 = \overline{I}_5 - \overline{I}_2\overline{I}_3/\overline{I}_1, \qquad \overline{\overline{I}}_3^* = \overline{I}_5^* - \overline{I}_2^*\overline{I}_3^*/\overline{I}_1^*\\
&\overline{\overline{I}}_3 = (\overline{I}_3)^2/\overline{I}_1 - c_1^2 I_7, \qquad \overline{\overline{I}}_3^* = (\overline{I}_3^*)^2/\overline{I}_1^* - c_1^2 I_7
\end{aligned} \tag{24}$$

Inserting Eqs. (11), (13) into Eq. (17) and then into Eqs. (23) gives

$$
\begin{aligned}
&L_{11}(w)+L_{12}(\phi_x)+L_{13}(\phi_y)+L_{14}(f)+S(w,f)+q\\
&\quad=I_1\frac{\partial^2 w}{\partial t^2}+2\varepsilon I_1\frac{\partial w}{\partial t}+\overline{\overline{I}}_5\frac{\partial^3\phi_x}{\partial t^2\partial x}+\overline{\overline{I}}^*_5\frac{\partial^3\phi_y}{\partial t^2\partial y}\\
&\qquad+\overline{\overline{I}}_7\frac{\partial^4 w}{\partial t^2\partial x^2}+\overline{\overline{I}}^*_7\frac{\partial^4 w}{\partial t^2\partial y^2}\\
&L_{21}(w)+L_{22}(\phi_x)+L_{23}(\phi_y)+L_{24}(f)=\overline{\overline{I}}_3\frac{\partial^2\phi_x}{\partial t^2}-\overline{\overline{I}}_5\frac{\partial^3 w}{\partial t^2\partial x}\\
&L_{31}(w)+L_{32}(\phi_x)+L_{33}(\phi_y)+L_{34}(f)=\overline{\overline{I}}^*_3\frac{\partial^2\phi_y}{\partial t^2}-\overline{\overline{I}}^*_5\frac{\partial^3 w}{\partial t^2\partial y}
\end{aligned}
\tag{25}
$$

in which

$$
\begin{aligned}
L_{11}(w)&=X_{11}\frac{\partial^2 w}{\partial x^2}+X_{12}\frac{\partial^2 w}{\partial y^2}+X_{13}\frac{\partial^4 w}{\partial x^4}+X_{14}\frac{\partial^4 w}{\partial x^2\partial y^2}\\
&\quad+X_{15}\frac{\partial^4 w}{\partial y^4}-k_1 w+k_2\left(\frac{\partial^2 w}{\partial x^2}+\frac{\partial^2 w}{\partial y^2}\right)\\
L_{12}(\phi_x)&=X_{11}\frac{\partial\phi_x}{\partial x}+X_{16}\frac{\partial^3\phi_x}{\partial x^3}+X_{17}\frac{\partial^3\phi_x}{\partial x\partial y^2},\\
L_{13}(\phi_y)&=X_{12}\frac{\partial\phi_y}{\partial y}+X_{18}\frac{\partial^3\phi_y}{\partial y^3}+X_{19}\frac{\partial^3\phi_y}{\partial x^2\partial y}\\
L_{14}(f)&=X_{110}\frac{\partial^4 f}{\partial x^4}+X_{111}\frac{\partial^4 f}{\partial x^2\partial y^2}+X_{112}\frac{\partial^4 f}{\partial y^4}\\
S(w,f)&=\frac{\partial^2 f}{\partial y^2}\frac{\partial^2 w}{\partial x^2}-2\frac{\partial^2 f}{\partial x\partial y}\frac{\partial^2 w}{\partial y^2}+\frac{\partial^2 f}{\partial x^2}\frac{\partial^2 w}{\partial y^2}\\
&\quad+\frac{1}{R_x}\frac{\partial^2 f}{\partial x^2}+\frac{1}{R_y}\frac{\partial^2 f}{\partial y^2}\\
L_{21}(w)&=X_{21}\frac{\partial w}{\partial x}+X_{22}\frac{\partial^3 w}{\partial x^3}+X_{23}\frac{\partial^3 w}{\partial x\partial y^2},\\
L_{22}(\phi_x)&=X_{21}\phi_x+X_{24}\frac{\partial^2\phi_x}{\partial x^2}+X_{25}\frac{\partial^2\phi_x}{\partial y^2}\\
L_{23}(\phi_y)&=X_{26}\frac{\partial^2\phi_y}{\partial x\partial y},\qquad L_{24}(f)=X_{27}\frac{\partial^3 f}{\partial x^3}+X_{28}\frac{\partial^3 f}{\partial x\partial y^2}\\
L_{31}(w)&=X_{31}\frac{\partial w}{\partial y}+X_{32}\frac{\partial^3 w}{\partial x^2\partial y}+X_{33}\frac{\partial^3 w}{\partial y^3},\\
L_{32}(\phi_x)&=X_{34}\frac{\partial^2\phi_x}{\partial x\partial y}\\
L_{33}(\phi_y)&=X_{31}\phi_y+X_{35}\frac{\partial^2\phi_y}{\partial x^2}+X_{36}\frac{\partial^2\phi_y}{\partial y^2},\\
L_{34}(f)&=X_{37}\frac{\partial^3 f}{\partial x^2\partial y}+X_{38}\frac{\partial^3 f}{\partial y^3}
\end{aligned}
\tag{26}
$$

and the detail of coefficients X_{1i} $(i=\overline{1,12})$, X_{2j} $(j=\overline{1,8})$, X_{3k} $(k=\overline{1,8})$ may be found in Appendix A.

For an imperfect FG-CNTRC double curved shallow shell, Eqs. (26) may be transformed to the form as

$$
\begin{aligned}
&L_{11}(w)+L_{12}(\phi_x)+L_{13}(\phi_y)+L_{14}(f)+S(w,f)\\
&\quad+S^*\left(w^*,f\right)+q=I_1\frac{\partial^2 w}{\partial t^2}+2\varepsilon I_1\frac{\partial w}{\partial t}\\
&\quad+\overline{\overline{I}}_5\frac{\partial^3\phi_x}{\partial t^2\partial x}+\overline{\overline{I}}^*_5\frac{\partial^3\phi_y}{\partial t^2\partial y}+\overline{\overline{I}}_7\frac{\partial^4 w}{\partial t^2\partial x^2}+\overline{\overline{I}}^*_7\frac{\partial^4 w}{\partial t^2\partial y^2}\\
&L_{21}(w)+L_{22}(\phi_x)+L_{23}(\phi_y)+L_{24}(f)+L^*_{21}\left(w^*\right)\\
&\quad=\overline{\overline{I}}_3\frac{\partial^2\phi_x}{\partial t^2}-\overline{\overline{I}}_5\frac{\partial^3 w}{\partial t^2\partial x}\\
&L_{31}(w)+L_{32}(\phi_x)+L_{33}(\phi_y)+L_{34}(f)+L^*_{31}\left(w^*\right)\\
&\quad=\overline{\overline{I}}^*_3\frac{\partial^2\phi_y}{\partial t^2}-\overline{\overline{I}}^*_5\frac{\partial^3 w}{\partial t^2\partial y}
\end{aligned}
\tag{27}
$$

in which

$$
\begin{aligned}
L^*_{11}\left(w^*\right)&=X_{11}\frac{\partial^2 w^*}{\partial x^2}+X_{12}\frac{\partial^2 w^*}{\partial y^2},\\
S^*\left(w^*,f\right)&=\frac{\partial^2 f}{\partial y^2}\frac{\partial^2 w^*}{\partial x^2}-2\frac{\partial^2 f}{\partial x\partial y}\frac{\partial^2 w^*}{\partial x\partial y}+\frac{\partial^2 f}{\partial x^2}\frac{\partial^2 w^*}{\partial y^2}\\
L^*_{21}\left(w^*\right)&=X_{21}\frac{\partial w^*}{\partial x},\qquad L^*_{31}\left(w^*\right)=X_{31}\frac{\partial w^*}{\partial y}
\end{aligned}
\tag{28}
$$

Introduction of Eqs. (19) into Eq. (7) gives the compatibility equation of the imperfect FG-CNTRC double curved shallow shell as

$$
\begin{aligned}
&I_{21}\frac{\partial^4 f}{\partial x^4}+I_{11}\frac{\partial^4 f}{\partial y^4}+J_1\frac{\partial^4 f}{\partial x^2\partial y^2}+J_2\frac{\partial^3\phi_x}{\partial x^3}+J_3\frac{\partial^3\phi_x}{\partial x\partial y^2}\\
&\quad+J_4\frac{\partial^3\phi_y}{\partial y^3}+J_5\frac{\partial^3\phi_y}{\partial y\partial x^2}-c_1 I_{25}\frac{\partial^4 w}{\partial x^4}-c_1 I_{16}\frac{\partial^4 w}{\partial y^4}\\
&\quad+J_6\frac{\partial^4 w}{\partial x^2\partial y^2}-\left(\frac{\partial^2 w^2}{\partial x\partial y}-\frac{\partial^2 w}{\partial x^2}\frac{\partial^2 w}{\partial y^2}+2\frac{\partial^2 w}{\partial x\partial y}\frac{\partial^2 w^*}{\partial x\partial y}\right.\\
&\quad\left.-\frac{\partial^2 w}{\partial x^2}\frac{\partial^2 w^*}{\partial y^2}-\frac{\partial^2 w}{\partial y^2}\frac{\partial^2 w^*}{\partial x^2}-\frac{1}{R_y}\frac{\partial^2 w}{\partial x^2}-\frac{1}{R_x}\frac{\partial^2 w}{\partial y^2}\right)=0
\end{aligned}
\tag{29}
$$

where

$$
\begin{aligned}
&J_1=I_{31}-2I_{12},\qquad J_2=I_{23}-c_1 I_{25},\\
&J_3=I_{13}-c_1 I_{15}-I_{32}+c_1 I_{33}\\
&J_4=I_{14}-c_1 I_{16},\qquad J_5=I_{24}-c_1 I_{26}-I_{32}+c_1 I_{33},\\
&J_6=-c_1 I_{15}-c_1 I_{26}+2c_1 I_{33}
\end{aligned}
\tag{30}
$$

Eqs. (27) and (29) are nonlinear equations in term of variables w,ϕ_x,ϕ_y and f and used to investigate the vibration of imperfect FG-CNTRC double curved shallow shells under blast and thermal loads using the third order shear theory.

4. Solution procedure

The imperfect FG-CNTRC double curved shallow shell is assumed to be simply supported and subjected to blast load q. Four edges of the shell are simply supported and immovable. The boundary conditions are

$$
\begin{aligned}
&w=u=\phi_y=M_x=P_x=0,\qquad N_x=N_{x0}\quad \text{at } x=0,a\\
&w=v=\phi_x=M_y=P_y=0,\qquad N_y=N_{y0}\quad \text{at } y=0,b
\end{aligned}
\tag{31}
$$

where N_{x0}, N_{y0} are fictitious compressive edge loads at immovable edges.

The mentioned conditions (31) can be satisfied identically if the approximate solutions are chosen by [25,33,39]

$$
\begin{bmatrix} w(x,y,t)\\ \phi_x(x,y,t)\\ \phi_y(x,y,t)\end{bmatrix}=\begin{bmatrix} W(t)\sin\lambda_m x\sin\delta_n y\\ \Phi_x(t)\cos\lambda_m x\sin\delta_n y\\ \Phi_y(t)\sin\lambda_m x\cos\delta_n y\end{bmatrix}
\tag{32}
$$

where $\lambda_m=m\pi/a$, $\delta_n=n\pi/b$; m,n are odd natural numbers representing the number of half waves in the x and y directions, respectively; and $W(t),\Phi_x,\Phi_y$ are the time dependent amplitudes.

Concerning with the initial imperfection w^* we introduce an assumption, it has the form like the shell deflection, i.e.

$$
w^*(x,y)=\mu h\sin\lambda_m x\sin\delta_n y
\tag{33}
$$

in which μ is imperfection parameter of the shell.

Introducing Eqs. (32) and (33) into the compatibility equation (29) and solving obtained equation for unknown f leads to

$$f = A_1(t)\cos 2\lambda_m x + A_2(t)\cos 2\delta_n y + A_3(t)\sin\lambda_m x \sin\delta_n y + \frac{1}{2}N_{x0}y^2 + \frac{1}{2}N_{y0}x^2 \tag{34}$$

with

$$\begin{aligned} A_1 &= \frac{\delta_n^2}{32I_{21}\lambda_m^2}W(W+2\mu h),\\ A_2 &= \frac{\lambda_m^2}{32I_{11}\delta_n^2}W(W+2\mu h),\\ P_3 &= Q_1 W + Q_2\Phi_x + Q_3\Phi_y \end{aligned} \tag{35}$$

and

$$\begin{aligned} Q_1 &= \frac{(\frac{\delta_n^2}{R_x}+\frac{\lambda_m^2}{R_y}) + c_1 I_{25}\lambda_m^4 + c_1 I_{16}\delta_n^4 - J_6\lambda_m^2\delta_n^2}{I_{21}\lambda_m^4 + J_1\lambda_m^2\delta_n^2 + I_{11}\delta_n^4},\\ Q_2 &= \frac{-(J_2\lambda_m^3 + J_3\lambda_m\delta_n^2)}{I_{21}\lambda_m^4 + J_1\lambda_m^2\delta_n^2 + I_{11}\delta_n^4},\\ Q_3 &= \frac{-(J_4\delta_n^3 + J_5\lambda_m^2\delta_n)}{I_{21}\lambda_m^4 + J_1\lambda_m^2\delta_n^2 + I_{11}\delta_n^4} \end{aligned} \tag{36}$$

Replacing Eqs. (32)–(34) into Eqs. (27) and then applying Galerkin method to the resulting equations yields

$$\begin{aligned} &l_{11}W + l_{12}\Phi_x + l_{13}\Phi_y + l_{14}(W+\mu h)\Phi_x + l_{15}(W+\mu h)\Phi_y\\ &\quad + \left[n_1 - \left(N_{x0}\lambda_m^2 + N_{y0}\delta_n^2\right)\right](W+\mu h)\\ &\quad + n_2 W(W+\mu h) + n_3 W(W+2\mu h)\\ &\quad + n_4 W(W+\mu h)(W+2\mu h)\\ &\quad + n_5 q + n_5\left(\frac{N_{x0}}{R_x} + \frac{N_{y0}}{R_y}\right) = I_0\frac{\partial^2 W}{\partial t^2} + 2\varepsilon I_1\frac{\partial W}{\partial t}\\ &\quad - \lambda_m\overline{\overline{I}}_5\frac{\partial^2\Phi_x}{\partial t^2} - \delta_n\overline{\overline{I}}_5^*\frac{\partial^2\Phi_y}{\partial t^2}\\ &l_{21}W + l_{22}\Phi_x + l_{23}\Phi_y + n_6(W+\mu h) + n_7 W(W+2\mu h)\\ &\quad = \overline{\overline{I}}_3\frac{\partial^2\Phi_x}{\partial t^2} - \lambda_m\overline{\overline{I}}_5\frac{\partial^2 W}{\partial t^2}\\ &l_{31}W + l_{32}\Phi_x + l_{33}\Phi_y + n_8(W+\mu h) + n_9 W(W+2\mu h)\\ &\quad = \overline{\overline{I}}_3^*\frac{\partial^2\Phi_y}{\partial t^2} - \delta_n\overline{\overline{I}}_5^*\frac{\partial^2 W}{\partial t^2} \end{aligned} \tag{37}$$

in which the detail of coefficients l_{1i} $(i=\overline{1,5})$, l_{jk} $(j=\overline{2,3}, k=\overline{1,3})$, n_m $(m=\overline{1,9})$ may be found in Appendix B.

A simply supported FG-CNTRC double curved shallow shell on elastic foundations with all immovable edges is considered. The shell is subjected to blast load q (Pascals) and simultaneously exposed to temperature environments. The in-plane condition on immovability at all edges, i.e. $u=0$ at $x=0,a$ and $v=0$ at $y=0,b$, is fulfilled in an average sense as [25,33,39,42]

$$\int_0^b\int_0^a \frac{\partial u}{\partial x}dxdy = 0, \qquad \int_0^a\int_0^b \frac{\partial v}{\partial y}dydx = 0 \tag{38}$$

Form Eqs. (11) and (19) one can obtain the following expressions in which initial imperfection have been included

$$\begin{aligned} \frac{\partial u}{\partial x} &= I_{11}\frac{\partial^2 f}{\partial y^2} - I_{12}\frac{\partial^2 f}{\partial x^2} + I_{13}\frac{\partial\phi_x}{\partial x} + I_{14}\frac{\partial\phi_y}{\partial y}\\ &\quad - c_1 I_{15}\left(\frac{\partial^2 w}{\partial x^2} + \frac{\partial\phi_x}{\partial x}\right) - c_1 I_{16}\left(\frac{\partial^2 w}{\partial y^2} + \frac{\partial\phi_y}{\partial y}\right)\\ &\quad + I_{17}\Phi_1 + I_{18}\Phi_2 + \frac{w}{R_x} - \frac{1}{2}\left(\frac{\partial w}{\partial x}\right) - \frac{\partial w}{\partial x}\frac{\partial w^*}{\partial x}\\ \frac{\partial v}{\partial y} &= I_{21}\frac{\partial^2 f}{\partial x^2} - I_{12}\frac{\partial^2 f}{\partial y^2} + I_{23}\frac{\partial\phi_x}{\partial x} + I_{24}\frac{\partial\phi_y}{\partial y}\\ &\quad - c_1 I_{25}\left(\frac{\partial^2 w}{\partial x^2} + \frac{\partial\phi_x}{\partial x}\right) - c_1 I_{26}\left(\frac{\partial^2 w}{\partial y^2} + \frac{\partial\phi_y}{\partial y}\right)\\ &\quad + I_{27}\Phi_1 + I_{28}\Phi_2 + \frac{w}{R_y} - \frac{1}{2}\left(\frac{\partial w}{\partial y}\right) - \frac{\partial w}{\partial y}\frac{\partial w^*}{\partial y} \end{aligned} \tag{39}$$

Introduction of Eqs. (32)–(34) into Eq. (39) and then the result into Eq. (38) gives

$$\begin{aligned} N_{x0} &= m_1 W + m_2\Phi_x + m_3\Phi_y + m_4 W(W+2\mu h)\\ &\quad + m_5\Phi_1 + m_6\Phi_2\\ N_{y0} &= m_1^* W + m_2^*\Phi_x + m_3^*\Phi_y + m_4^* W(W+2\mu h)\\ &\quad + m_5^*\Phi_1 + m_6^*\Phi_2 \end{aligned} \tag{40}$$

in which the details of m_i $(i=\overline{1,6})$ and m_j^* $(j=\overline{1,6})$ may be found in Appendix C.

Introduction of Eqs. (40) into Eq. (37), we have

$$\begin{aligned} &r_{11}W + r_{12}\Phi_x + r_{13}\Phi_y + r_{14}(W+\mu h)\Phi_x + r_{15}(W+\mu h)\Phi_y\\ &\quad + s_1(W+\mu h) + s_2 W(W+\mu h) + s_3 W(W+2\mu h)\\ &\quad + s_4 W(W+\mu h)(W+2\mu h) + n_5 q + s_5\\ &\quad = I_0\frac{\partial^2 W}{\partial t^2} + 2\varepsilon I_1\frac{\partial W}{\partial t} - \lambda_m\overline{\overline{I}}_5\frac{\partial^2\Phi_x}{\partial t^2} - \delta_n\overline{\overline{I}}_5^*\frac{\partial^2\Phi_y}{\partial t^2}\\ &l_{21}W + l_{22}\Phi_x + l_{23}\Phi_y + n_6(W+\mu h) + n_7 W(W+2\mu h)\\ &\quad = \overline{\overline{I}}_3\frac{\partial^2\Phi_x}{\partial t^2} - \lambda_m\overline{\overline{I}}_5\frac{\partial^2 W}{\partial t^2}\\ &l_{31}W + l_{32}\Phi_x + l_{33}\Phi_y + n_8(W+\mu h) + n_9 W(W+2\mu h)\\ &\quad = \overline{\overline{I}}_3^*\frac{\partial^2\Phi_y}{\partial t^2} - \delta_n\overline{\overline{I}}_5^*\frac{\partial^2 W}{\partial t^2} \end{aligned} \tag{41}$$

with

$$\begin{aligned} &r_{11} = l_{11} + \frac{n_5 m_1}{R_x} + \frac{n_5 m_1^*}{R_y}, \qquad r_{12} = l_{12} + \frac{n_5 m_2}{R_x} + \frac{n_5 m_2^*}{R_y},\\ &r_{13} = l_{13} + \frac{n_5 m_3}{R_x} + \frac{n_5 m_3^*}{R_y} \qquad r_{14} = l_{14} - m_2\lambda_m^2 - m_2^*\delta_n^2,\\ &r_{15} = l_{15} - m_3\lambda_m^2 - m_3^*\delta_n^2, \qquad s_1 = n_1 - \left(m_5 + m_5^*\right)\lambda_m^2\Phi_1\\ &-\left(m_6 + m_6^*\right)\delta_n^2\Phi_2, \qquad s_2 = n_2 - m_1\lambda_m^2 - m_1^*\delta_n^2,\\ &s_3 = n_3 + \frac{n_5 m_4}{R_x} + \frac{n_5 m_4^*}{R_y} \qquad s_4 = n_4 - m_4\lambda_m^2 - m_4^*\delta_n^2,\\ &s_5 = \frac{n_5(m_5\Phi_1 + m_6\Phi_2)}{R_x} + \frac{n_5(m_5^*\Phi_1 + m_6^*\Phi_2)}{R_y} \end{aligned} \tag{42}$$

This is basic equation governing of the nonlinear vibration for imperfect FG-CNTRC double curved shallow shells with immovable edges subjected to blast and thermal loads. It is solved by using the fourth-order Runge–Kutta method.

In the case of $q=0$, the natural frequencies of the perfect shell can be determined by solving the following equation

$$\begin{vmatrix} r_{11}+s_1+I_0\omega^2 & r_{12}-\lambda_m\overline{\overline{I}}_5\omega^2 & r_{13}-\delta_n\overline{\overline{I}}_5^*\omega^2\\ l_{21}+n_6-\lambda_m\overline{\overline{I}}_5\omega^2 & l_{22}+\overline{\overline{I}}_3\omega^2 & l_{23}\\ l_{31}+n_8-\delta_n\overline{\overline{I}}_5^*\omega^2 & l_{32} & l_{33}+\overline{\overline{I}}_3^*\omega^2 \end{vmatrix} = 0 \tag{43}$$

Table 2
Comparison of linear frequencies for isotropic cylindrical panels ($a = 0.2794$ m, $b = 0.2286$ m).

R (m)	h (mm)	(m, n)	Bardell and Mead [36]	Chern and Chao [37]	Shen and Xiang [13]	Present
2.4384	0.7112	(1, 1)	143.8	142.1	143.8	144.2
2.4384	1.2190	(1, 1)	163.1	161.4	163.2	164.4
1.8288	0.7112	(1, 2)	167.2	166.7	167.4	168.5
1.8288	1.2190	(1, 1)	200.8	198.5	200.8	201.5
1.2192	0.7112	(1, 2)	181.6	180.8	181.7	182.8
1.2192	1.2190	(1, 2)	281.8	278.1	281.9	283.1

Table 3
Comparison of the dimensionless frequencies $\Omega = \omega h\sqrt{\rho_c/E_c}$ for Al/Al_2O_3 FGM cylindrical panels.

b/R		N				
		0	0.5	1	4	10
0.5	Matsunaga [38]	0.2153	0.1855	0.1678	0.1413	0.1328
	Aragh et al. [10]	0.2129	0.1817	0.1638	0.1374	0.1296
	Shen and Xiang [13]	0.2169	0.1799	0.1589	0.1301	0.1204
	Present	0.2186	0.1864	0.1701	0.1421	0.1335
1.0	Matsunaga [38]	0.2239	0.1945	0.1769	0.1483	0.1380
	Aragh et al. [10]	0.2154	0.1848	0.1671	0.1391	0.1300
	Shen and Xiang [13]	0.2329	0.1944	0.1732	0.1402	0.1286
	Present	0.2335	0.1970	0.1792	0.1482	0.1395

5. Numerical results and discussion

5.1. Validation of the present study

In order to validate the accuracy of the present method, the linear frequencies of isotropic cylindrical panel and the dimensionless frequencies of FGM cylindrical panel are compared with other results obtained by other authors.

Firstly, Table 2 shows the comparison of the linear frequencies $f = \omega/2\pi$ (Hz) for isotropic cylindrical panels ($a = 0.2794$ m, $b = 0.2286$ m) in this paper with the results presented by Bardell and Mead [36] based on the hierarchical finite element method, Chern and Chao [37] using the three-dimensional theory and Shen and Xiang [13] with the higher order shear theory. The mechanical properties are chosen as $E = 72$ GPa, $\nu = 1/3$, $\rho = 2800$ kg/m^3. From the Table 2, good agreements are observed for the present solution and the numerical results of three publications.

Next, the values of the dimensionless frequencies $\Omega = \omega h\sqrt{\rho_c/E_c}$ for Al/Al_2O_3 FGM cylindrical panels are calculated and compared in Table 3 with the 2-D higher order deformation theory solutions of Matsunaga [38], the differential quadrature method results of Aragh et al. [10] and the higher order shear theory solutions of Shen and Xiang [13]. The input data are $a/b = 1, b/h = 5, E_{11}/E_{22} = 25, G_{12} = G_{13} = 0.5E_{22}, G_{23} = 0.2E_{22}, \nu_{12} = 0.25$ and $\rho = 1$. Again, this comparison study also show that the present results agree very well the existing results.

5.2. Natural frequency

The effects of CNT volume fraction V^*_{CNT}, temperature increment ΔT and types of FG-CNTRCs on the natural oscillation frequency of the FG-CNTRC double curved shallow shell subjected to blast and thermal loads with $b/a = 1, b/h = 20, R_x/h = R_y/h = 1500, \mu = 0.1$ are shown in Table 4. It is easy to see that the value of the natural oscillation frequency increases when the value of CNT volume fraction increases and the value of temperature increment decreases. The Table 4 also shows that natural oscillation frequency of FGX-CNTRC double curved shallow shell is higher than that of FGV-CNTRC double curved shallow shell which is also higher than the frequency of FGO-CNTRC double curved shallow shell.

Table 5 illustrates the influences of elastic foundations, geometrical parameter a/h, CNT volume fraction and types of FG-CNTRCs on the natural frequencies of the imperfect FG-CNTRC double curved shallow shells with immovable edges under blast and thermal loads. First, the natural frequencies of FG-CNTRC double curved shallow shell of type X is highest and the natural frequencies of FG-CNTRC double curved shallow shell of type O is lowest of all. Furthermore, increases of two coefficients k_1, k_2 of elastic foundations and decreases of CNT volume fraction, ratio a/h lead to increases of the natural frequencies of FG-CNTRC double curved shallow shell.

5.3. Nonlinear dynamic response

Figs. 2, 3 indicate effects of elastic foundations with two coefficients k_1, k_2 on the dynamic response of the imperfect FG-CNTRC double curved shallow shells subjected to blast and thermal loads. As can be observed, the FG-CNTRC double curved shallow shell fluctuation amplitude decreased significantly due to the support of elastic foundations. Moreover, the beneficial effect of the Pasternak foundation with the shear layer stiffness k_2 on the dynamic response of the imperfect FG-CNTRC double curved shallow shells is stronger than the Winkler one with the modulus k_1. One special point is that in all figures of nonlinear dynamic response, due to the presence of blast load, the oscillation of FG-CNTRC double curved shallow shell is damped. Furthermore, the dynamic response of FG-CNTRC double curved shallow shell from Fig. 2 to Fig. 9 is investigated for type X.

Fig. 4 shows effect of temperature increment ΔT on the nonlinear dynamic response of the imperfect FG-CNTRC double curved shallow shells subjected to blast and thermal loads. Obviously, an increase of temperature increment leads to the rise of the fluctuation amplitude of the shell.

The influences of initial imperfection with imperfection coefficient μ on the nonlinear dynamic response of FG-CNTRC double curved shallow shells subjected to blast and thermal loads are shown in Fig. 5. Three values of μ: 0, 0.1 and 0.3 are used. It can be seen that the amplitude of the FG-CNTRC double curved shallow shell increased when the coefficient μ increased.

Figs. 6–8 consider the effects of geometrical parameters $b/a, b/h$ and R_x/h on the nonlinear dynamic response of imperfect FG-CNTRC double curved shallow shells subjected to blast and thermal loads, respectively. The results from these figures show that the fluctuation amplitude of the imperfect FG-CNTRC double curved

Table 4
Effects of CNT volume fraction, types of FG-CNTRCs and temperature increment on natural frequencies (s^{-1}) of the FG-CNTRC double curved shallow shell.

ΔT (K)	$V^*_{CNT} = 0.12$			$V^*_{CNT} = 0.17$			$V^*_{CNT} = 0.28$		
	FG-O	FG-V	FG-X	FG-O	FG-V	FG-X	FG-O	FG-V	FG-X
0	1094	1123	1128	1137	1198	1221	1145	1206	1232
100	1052	1070	1085	1074	1120	1127	1094	1146	1157
200	1014	1020	1045	1025	1043	1067	1036	1062	1085
400	956	972	981	975	995	1017	992	1024	1063
600	931	949	964	966	991	998	973	996	1023

Table 5
Effects of elastic foundations, ratio a/h, CNT volume fraction and types of FG-CNTRCs on natural frequencies (s^{-1}) of the FG-CNTRC double curved shallow shell.

(k_1 (GPa/m), k_2 (GPa.m))	a/h	$V^*_{CNT} = 0.12$			$V^*_{CNT} = 0.17$		
		FG-O	FG-V	FG-X	FG-O	FG-V	FG-X
(0, 0)	20	198	213	225	253	338	420
(0, 0)	30	142	168	176	236	284	317
(0, 0)	40	136	155	164	224	271	318
(0.1, 0.02)	20	887	903	925	883	932	972
(0.1, 0.02)	30	695	740	786	746	769	824
(0.1, 0.02)	40	671	692	743	675	718	804

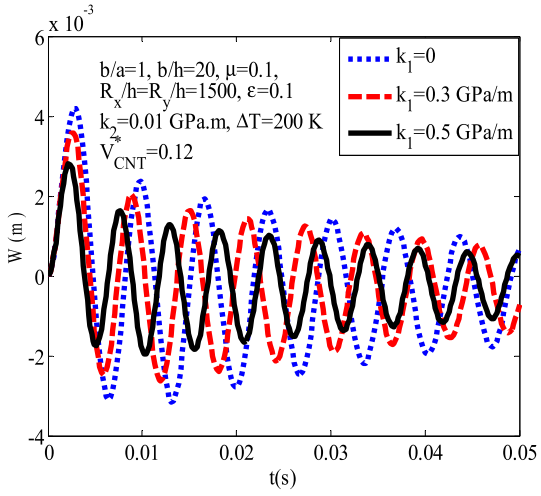

Fig. 2. Effects of the linear Winkler foundation on the nonlinear dynamic response of the imperfect FG-CNTRC double curved shallow shell subjected to blast and thermal loads.

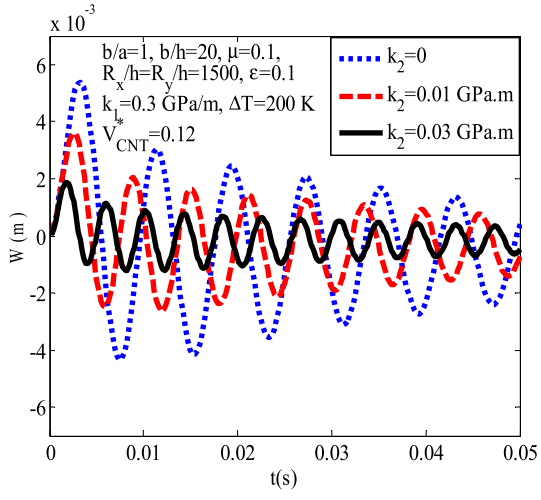

Fig. 3. Effects of the Pasternak foundation on the nonlinear dynamic response of the imperfect FG-CNTRC double curved shallow shell subjected to blast and thermal loads.

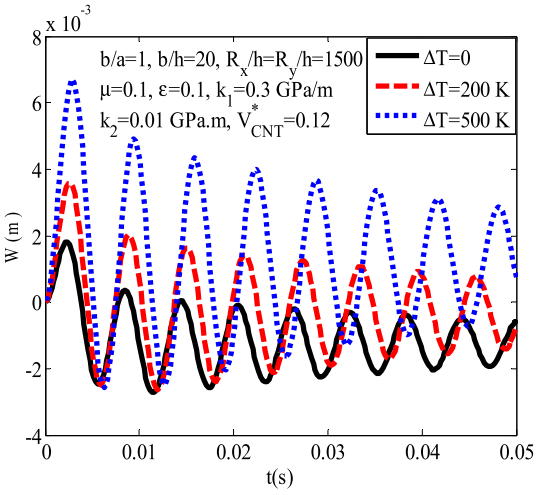

Fig. 4. Effects of temperature increment on the nonlinear dynamic response of the imperfect FG-CNTRC double curved shallow shell subjected to blast and thermal loads.

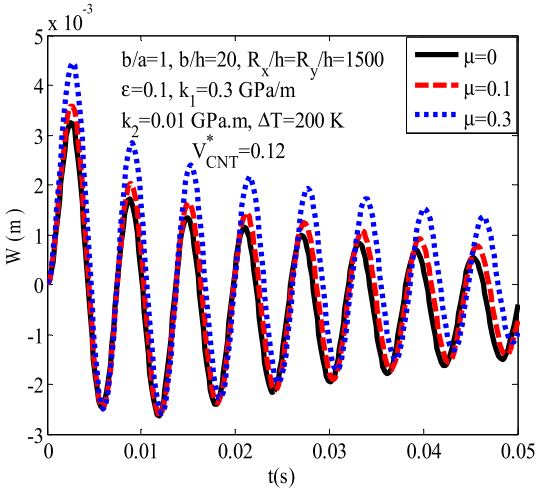

Fig. 5. Effects of initial imperfection on the nonlinear dynamic response of the imperfect FG-CNTRC double curved shallow shell subjected to blast and thermal loads.

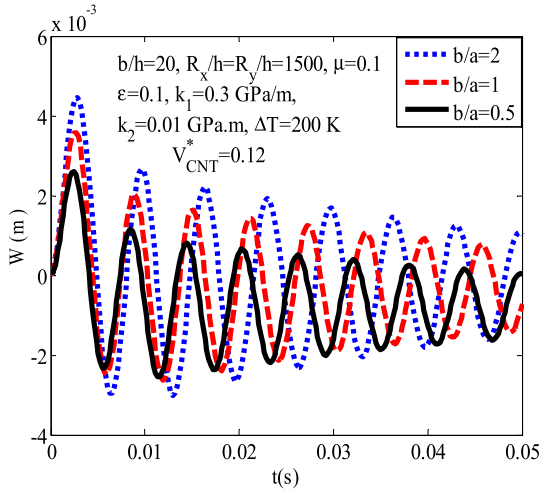

Fig. 6. Effects of ratio b/a on the nonlinear dynamic response of the imperfect FG-CNTRC double curved shallow shell subjected to blast and thermal loads.

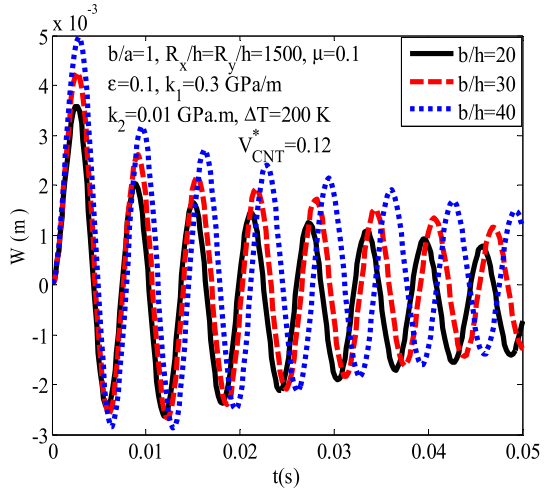

Fig. 7. Effects of ratio b/h on the nonlinear dynamic response of the imperfect FG-CNTRC double curved shallow shell subjected to blast and thermal loads.

shallow shells decreased when decreasing the ratio $b/a, b/h$ and increasing the ratio R_x/h.

Fig. 9 illustrates the nonlinear dynamic response of the imperfect FG-CNTRC double curved shallow shells subjected to the combination of blast and thermal loads with different carbon nanotube volume fraction (V^*_{CNT}). From the obtained results, we can see that the higher the carbon nanotube volume fraction is, the lower the amplitude of the FG-CNTRC double curved shallow shells is. This is reasonable to the fact that the stiffness of FG-CNTRC double curved shallow shells is larger when the proportion of CNTs by volume is higher.

Comparison of the amplitude fluctuation for FG-CNTRC double curved shallow shells of type X, V and O subjected to blast and thermal loads with the same geometrical dimensions is given in Fig. 10. As expected, the amplitude fluctuation of FG-CNTRC double curved shallow shell of type O is highest and the amplitude fluctuation of FG-CNTRC double curved shallow shell of type X is lowest of all.

6. Concluding remarks

This paper used successfully analytical approach to investigate the nonlinear vibration of imperfect thick FG-CNTRC double curved shallow shells. The shell is assumed to rest on elastic foundations

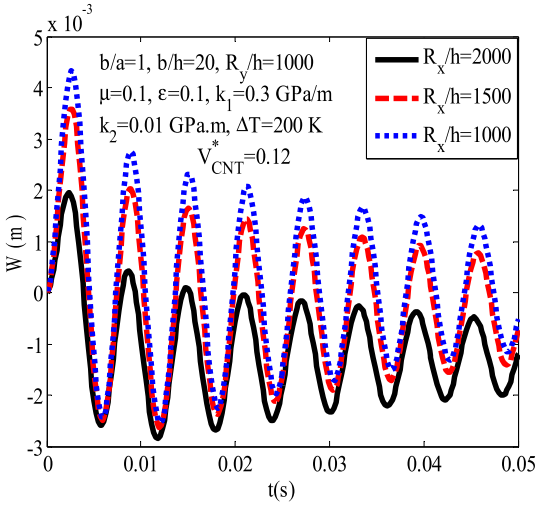

Fig. 8. Effects of ratio R_x/h on the nonlinear dynamic response of the imperfect FG-CNTRC double curved shallow shell subjected to blast and thermal loads.

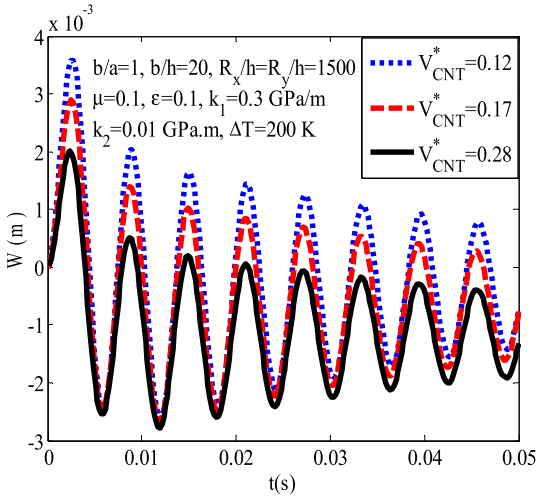

Fig. 9. Effects of CNT volume fraction on the nonlinear dynamic response of the imperfect FG-CNTRC double curved shallow shell subjected to blast and thermal loads.

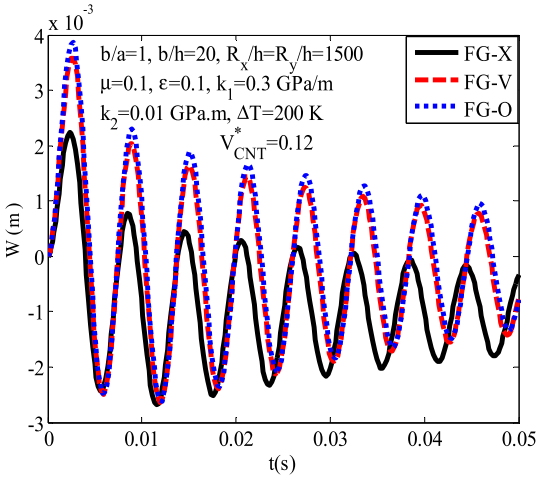

Fig. 10. The nonlinear dynamic response of the imperfect FG-CNTRC double curved shallow shell subjected to blast and thermal loads with different types of CNT reinforcements.

and subjected to blast load and temperature. The shell's properties depend on temperature and change according to the linear functions of the shell thickness. Governing equations are derived using the Airy stress function and higher order shear theory taking into account the effects of initial geometric imperfection. Then they are solved by Galerkin method and fourth-order Runge–Kutta method. The present numerical results are compared with other results obtained from the literature. Some conclusions can be obtained from the present analysis in this study:

(i) Carbon nanotube enhances the stiffness of FG-CNTRC double curved shallow shells.

(ii) The initial imperfection and temperature increment strongly negative influence on the vibration of the FG-CNTRC double curved shallow shell.

(iii) Elastic foundations have beneficial effect on the nonlinear dynamic response and natural frequencies of FG-CNTRC double curved shallow shells. Moreover, the influence of nonlinear Pasternalk foundation is stronger than linear Winkler foundation.

(iv) While comparing with the amplitude fluctuation of FG-CNTRC double curved shallow shell of type V, the amplitude fluctuation of FG-CNTRC double curved shallow shell of type O is higher and the amplitude fluctuation of FG-CNTRC double curved shallow shell of type X is lower.

(v) The geometrical parameters have significant influences on the nonlinear vibration of the FG-CNTRC shells.

The results achieved from stability analysis of FG-CNTRC structures will provide important data for designing and ensuring the appropriate structure in manufacturing and safety in using. Furthermore, achieved results are in the analytical form, so this study provides scientific foundations for designers, manufacturers in application using FG-CNTRCs. They are able to properly select the reasonable input parameters of the structures to create preeminent loads, thermal resistant capabilities, decrease the cracking and destroying FG-CNTRC structure under heavy loads.

Funding

This research is funded by Vietnam National Foundation for Science and Technology Development (NAFOSTED) under grant number 107.02-2015.03. The authors are grateful for this support.

Conflict of interest statement

The authors declare no conflict of interest.

Appendix A

$$
\begin{aligned}
X_{11} &= A_{44} - 6c_1D_{44} + 9c_1^2F_{44},\\
X_{12} &= A_{55} - 6c_1D_{55} + 9c_1^2F_{55},\\
X_{13} &= -c_1^2(E_{11}I_{15} + E_{12}I_{25} + H_{11})\\
X_{14} &= -c_1^2(4E_{66}I_{33} + 4H_{66} + E_{11}I_{16} + E_{12}I_{26} + 2H_{12}\\
&\quad + E_{12}I_{15} + E_{22}I_{25})\\
X_{15} &= -c_1^2(E_{12}I_{16} + E_{22}I_{26} + H_{22}),\\
X_{16} &= c_1(E_{11}I_{13} - c_1E_{11}I_{15} + F_{11} - c_1H_{11} + E_{12}I_{23} - c_1E_{12}I_{25})\\
X_{17} &= c_1(2E_{66}I_{32} - 2c_1E_{66}I_{33} + 2F_{66} - 2c_1H_{66} + c_1E_{12}I_{13}\\
&\quad - c_1E_{12}I_{15} + F_{12} - c_1H_{12} + E_{22}I_{23} - c_1E_{22}I_{25})\\
X_{18} &= c_1(E_{12}I_{14} - c_1E_{12}I_{16} + E_{22}I_{24} - c_1E_{22}I_{26} + F_{22}\\
&\quad - c_1H_{22}),\\
X_{19} &= c_1(2E_{66}I_{32} - 2c_1E_{66}I_{33} + 2F_{66} - 2c_1H_{66} + E_{11}I_{14}\\
&\quad - c_1E_{11}I_{16} + E_{12}I_{24} - c_1E_{12}I_{26} + F_{12} - c_1H_{12}),\\
X_{110} &= -c_1(E_{11}I_{12} - E_{12}I_{21})\\
X_{111} &= -c_1(2E_{66}I_{31} - E_{11}I_{11} + 2E_{12}I_{12} - E_{22}I_{21}),\\
X_{112} &= c_1(E_{12}I_{11} - E_{22}I_{12})\\
X_{21} &= -A_{44} + 6c_1D_{44} - 9c_1^2F_{44},\\
X_{22} &= -c_1(B_{11}I_{15} + F_{11} + B_{12}I_{25} - c_1E_{11}I_{15} - c_1H_{11}\\
&\quad - c_1E_{12}I_{25})\\
X_{23} &= -c_1(B_{11}I_{16} + B_{12}I_{26} + F_{12} + 2B_{66}I_{33} + 2F_{66} - 2c_1E_{66}I_{33}\\
&\quad - 2c_1H_{66} - c_1E_{11}I_{16} - c_1E_{12}I_{26} - c_1H_{12})\\
X_{24} &= B_{11}I_{13} - c_1B_{11}I_{15} + D_{11} - c_1F_{11} + B_{12}I_{23}\\
&\quad - c_1B_{12}I_{25} - c_1E_{11}I_{13} + c_1^2E_{11}I_{15} - c_1F_{11} + c_1^2H_{11}\\
&\quad - c_1E_{12}I_{23} + c_1^2E_{12}I_{25},\\
X_{25} &= B_{66}I_{32} - c_1B_{66}I_{33} + D_{66} - c_1F_{66} - c_1E_{66}I_{32}\\
&\quad + c_1^2E_{66}I_{33} - c_1F_{66} + c_1^2H_{66}\\
X_{26} &= B_{11}I_{14} - c_1B_{11}I_{16} + B_{12}I_{24} - c_1B_{12}I_{26} + D_{12} - c_1F_{12}\\
&\quad + B_{66}I_{32} - c_1B_{66}I_{33} + D_{66} - c_1F_{66} - c_1E_{66}I_{32}\\
&\quad + c_1^2E_{66}I_{33} - c_1F_{66} + c_1^2H_{66} - c_1E_{11}I_{14}\\
&\quad + c_1^2E_{11}I_{16} - c_1E_{12}I_{24} + c_1^2E_{12}I_{26} - c_1F_{12} + c_1^2H_{12}\\
X_{27} &= -B_{11}I_{12} + B_{12}I_{21} + c_1E_{11}I_{12} - c_1E_{12}I_{21},\\
X_{28} &= B_{11}I_{11} - B_{12}I_{12} - B_{66}I_{31} - c_1E_{11}I_{11} + c_1E_{12}I_{12}\\
&\quad + c_1E_{66}I_{31},\\
X_{31} &= -A_{55} + 6c_1D_{55} - 9c_1^2F_{55},\\
X_{32} &= -c_1(2B_{66}I_{33} + 2F_{66} + B_{12}I_{15} + F_{12} + B_{22}I_{25}\\
&\quad - 2c_1E_{66}I_{33} - 2c_1H_{66} - c_1E_{12}I_{15} - c_1H_{12} - c_1E_{22}I_{25}),\\
X_{33} &= -c_1(B_{12}I_{16} + B_{22}I_{26} + F_{22} - c_1E_{12}I_{16}\\
&\quad - c_1E_{22}I_{26} - c_1H_{22}),\\
X_{34} &= B_{66}I_{32} - c_1B_{66}I_{33} + D_{66} - c_1F_{66} + B_{12}I_{13} - c_1B_{12}I_{15}\\
&\quad + D_{12} - c_1F_{12} + B_{22}I_{23}\\
&\quad - c_1B_{22}I_{25} - c_1E_{66}I_{32} + c_1^2E_{66}I_{33} - c_1F_{66} + c_1^2H_{66}\\
&\quad - c_1E_{12}I_{13} + c_1^2E_{12}I_{15} - c_1F_{12} + c_1^2H_{12} - c_1E_{22}I_{23}\\
&\quad + c_1^2E_{22}I_{25},\\
X_{35} &= B_{66}I_{32} - c_1B_{66}I_{33} + D_{66} - c_1F_{66} - c_1E_{66}I_{32}\\
&\quad + c_1^2E_{66}I_{33} - c_1F_{66} + c_1^2H_{66}\\
X_{36} &= B_{12}I_{14} - c_1B_{12}I_{16} + B_{22}I_{24} - c_1B_{22}I_{26} + D_{22}\\
&\quad - c_1F_{22} - c_1E_{12}I_{14} + c_1^2E_{12}I_{16} - c_1E_{22}I_{24}\\
&\quad + c_1^2E_{22}I_{26} - c_1F_{22} + c_1^2H_{22},\\
X_{37} &= -B_{66}I_{31} - B_{12}I_{12} + B_{22}I_{21} + c_1E_{66}I_{31} + c_1E_{12}I_{12}\\
&\quad - c_1E_{22}I_{21}\\
X_{38} &= B_{12}I_{11} - B_{22}I_{12} - c_1E_{12}I_{11} + c_1E_{22}I_{12}
\end{aligned}
$$

Appendix B

$$
\begin{aligned}
l_{11} &= -k_1 - k_2\left(\lambda_m^2 + \delta_n^2\right) + X_{13}\lambda_m^4 + X_{14}\lambda_m^2\delta_n^2 + X_{15}\delta_n^4\\
&\quad + X_{110}Q_1\lambda_m^4 + X_{111}Q_1\lambda_m^2\delta_n^2 + X_{112}Q_1\delta_n^4\\
&\quad - Q_1\left(\frac{\lambda_m^2}{R_y} + \frac{\delta_n^2}{R_x}\right),
\end{aligned}
$$

$$l_{12} = -X_{11}\lambda_m + X_{16}\lambda_m^3 + X_{17}\lambda_m\delta_n^2 + X_{110}Q_2\lambda_m^4 + X_{111}Q_2\lambda_m^2\delta_n^2 + X_{112}Q_2\delta_n^4 - Q_2\left(\frac{\lambda_m^2}{R_y} + \frac{\delta_n^2}{R_x}\right),$$

$$l_{13} = -X_{12}\delta_n + X_{18}\delta_n^3 + X_{19}\lambda_m^2\delta_n + X_{110}Q_3\lambda_m^4 + X_{111}Q_3\lambda_m^2\delta_n^2 + X_{112}Q_3\delta_n^4 - Q_3\left(\frac{\lambda_m^2}{R_y} + \frac{\delta_n^2}{R_x}\right),$$

$$l_{14} = \frac{32Q_2\lambda_m\delta_n}{3ab}, \qquad l_{15} = \frac{32Q_3\lambda_m\delta_n}{3ab},$$

$$n_1 = -X_{11}\lambda_m^2 - X_{12}\delta_n^2, \qquad n_2 = \frac{32Q_1\lambda_m\delta_n}{3ab}$$

$$n_3 = \frac{2\delta_n}{3abI_{21}\lambda_m R_y} + \frac{2\lambda_m}{3abI_{11}\delta_n R_x} - \frac{8X_{110}\lambda_m\delta_n}{3abI_{21}} - \frac{8X_{112}\lambda_m\delta_n}{3abI_{11}},$$

$$n_4 = -\frac{\lambda_m^4}{16I_{11}} - \frac{\delta_n^4}{16I_{21}}, \qquad n_5 = \frac{16}{mn\pi^2}$$

$$l_{21} = -\lambda_m^3(X_{22} + Q_1X_{27}) - \lambda_m\delta_n^2(X_{23} + Q_1X_{28}),$$

$$l_{22} = X_{21} - X_{24}\lambda_m^2 - X_{25}\delta_n^2 - X_{27}Q_2\lambda_m^3 - X_{28}Q_2\lambda_m\delta_n^2$$

$$l_{23} = -X_{26}\lambda_m\delta_n - X_{27}Q_3\lambda_m^3 - X_{28}Q_3\lambda_m\delta_n^2,$$

$$n_6 = X_{21}\lambda_m, \qquad n_7 = \frac{8X_{27}\delta_n}{3abI_{21}},$$

$$l_{31} = -\delta_n^3(X_{33} + Q_1X_{38}) - \lambda_m^2\delta_n(X_{32} + Q_1X_{37}),$$

$$l_{32} = -X_{34}\lambda_m\delta_n - X_{38}Q_2\delta_n^3 - D_{37}Q_2\lambda_m^2\delta_n,$$

$$l_{33} = X_{31} - X_{35}\lambda_m^2 - X_{36}\delta_n^2 - X_{38}Q_3\delta_n^3 - X_{37}Q_3\lambda_m^2\delta_n,$$

$$n_8 = X_{31}\delta_n, \qquad n_9 = \frac{8X_{38}\lambda_3}{3abI_{11}}$$

Appendix C

$$m_1 = \frac{P_1I_{21} + P_4I_{12}}{I_{12}^2 - I_{11}I_{21}}, \qquad m_2 = \frac{P_2I_{21} + P_5I_{12}}{I_{12}^2 - I_{11}I_{21}},$$

$$m_3 = \frac{P_3I_{21} + P_6I_{12}}{I_{12}^2 - I_{11}I_{21}}, \qquad m_4 = \frac{I_{21}\lambda_m^2 + I_{12}\delta_n^2}{I_{12}^2 - I_{11}I_{21}}$$

$$m_5 = \frac{I_{17}I_{21} + I_{27}I_{12}}{I_{12}^2 - I_{11}I_{21}}, \qquad m_6 = \frac{I_{18}I_{21} + I_{28}I_{12}}{I_{12}^2 - I_{11}I_{21}},$$

$$m_1^* = \frac{P_1I_{12} + P_4I_{11}}{I_{12}^2 - I_{11}I_{21}}, \qquad m_2^* = \frac{P_2I_{12} + P_5I_{11}}{I_{12}^2 - I_{11}I_{21}}$$

$$m_3^* = \frac{P_3I_{12} + P_6I_{11}}{I_{12}^2 - I_{11}I_{21}}, \qquad m_4^* = \frac{I_{12}\lambda_m^2 + I_{11}\delta_n^2}{I_{12}^2 - I_{11}I_{21}},$$

$$m_5^* = \frac{I_{17}I_{12} + I_{27}I_{11}}{I_{12}^2 - I_{11}I_{21}}, \qquad m_6^* = \frac{I_{18}I_{12} + I_{28}I_{11}}{I_{12}^2 - I_{11}I_{21}}$$

$$P_1 = \frac{4Q_1(\frac{I_{12}\lambda_m}{\delta_n} - \frac{I_{11}\delta_n}{\lambda_m})}{ab} + \frac{4c_1(\frac{I_{15}\lambda_m}{\delta_n} + \frac{I_{16}\delta_n}{\lambda_m})}{ab} + \frac{4}{ab\lambda_m\delta_n R_x},$$

$$P_2 = \frac{4Q_2(\frac{I_{12}\lambda_m}{\delta_n} - \frac{I_{11}\delta_n}{\lambda_m})}{ab} - \frac{4I_{13}}{ab\delta_n} + \frac{4c_1I_{15}}{ab\delta_n},$$

$$P_3 = \frac{4Q_3(\frac{I_{12}\lambda_m}{\delta_n} - \frac{I_{11}\delta_n}{\lambda_m})}{ab} - \frac{4I_{14}}{ab\lambda_m} + \frac{4c_1I_{16}}{ab\lambda_m}$$

$$P_4 = \frac{4Q_1(\frac{I_{12}\delta_n}{\lambda_m} - \frac{I_{21}\lambda_m}{\delta_n})}{ab} + \frac{4c_1(\frac{I_{25}\lambda_m}{\delta_n} + \frac{I_{26}\delta_n}{\lambda_m})}{ab} + \frac{4}{ab\lambda_m\delta_n R_y},$$

$$P_5 = \frac{4Q_2(\frac{I_{12}\delta_n}{\lambda_m} - \frac{I_{21}\lambda_m}{\delta_n})}{ab} - \frac{4I_{23}}{ab\delta_n} + \frac{4c_1I_{25}}{ab\delta_n},$$

$$P_6 = \frac{4Q_3(\frac{I_{12}\delta_n}{\lambda_m} - \frac{I_{21}\lambda_m}{\delta_n})}{ab} - \frac{4I_{24}}{ab\lambda_m} + \frac{4I_{26}}{ab\lambda_m}$$

References

[1] L.W. Zhang, K.M. Liew, Postbuckling analysis of axially compressed CNT reinforced functionally graded composite plates resting on Pasternak foundations using an element-free approach, Compos. Struct. 138 (2016) 40–51.

[2] H.S. Shen, Thermal buckling and postbuckling behavior of functionally graded carbon nanotube-reinforced composite cylindrical shells, Composites, Part B, Eng. 43 (2012) 1030–1038.

[3] M. Griebel, J. Hamaekers, Molecular dynamics simulations of the elastic moduli of polymer–carbon nanotube composites, Comput. Methods Appl. Mech. Eng. 193 (2004) 1773–1788.

[4] R. Kolahchi, M.S. Zarei, M.H. Hajmohammad, A. Nouri, Wave propagation of embedded viscoelastic FG-CNT-reinforced sandwich plates integrated with sensor and actuator based on refined zigzag theory, Int. J. Mech. Sci. 130 (2017) 534–545.

[5] L.W. Zhang, W.C. Cui, K.M. Liew, Vibration analysis of functionally graded carbon nanotube reinforced composite thick plates with elastically restrained edges, Int. J. Mech. Sci. 103 (2015) 9–21.

[6] M. Mirzaei, Y. Kiani, Free vibration of functionally graded carbon nanotube reinforced composite cylindrical panels, Compos. Struct. 142 (2016) 45–56.

[7] R. Kolahchi, A comparative study on the bending, vibration and buckling of viscoelastic sandwich nano-plates based on different nonlocal theories using DC, HDQ and DQ methods, Aerosp. Sci. Technol. 66 (2017) 235–248.

[8] Y. Han, J. Elliott, Molecular dynamics simulations of the elastic properties of polymer/carbon nanotube composites, Comput. Mater. Sci. 39 (2007) 315–323.

[9] Z.G. Song, L.W. Zhang, K.M. Liew, Vibration analysis of CNT-reinforced functionally graded composite cylindrical shells in thermal environments, Int. J. Mech. Sci. 115 (116) (2016) 339–347.

[10] B.S. Aragh, A. Barati, H. Hedayati, Composites: Part B Eshelby–Mori–Tanaka approach for vibrational behavior of continuously graded carbon nanotube-reinforced cylindrical panels, Composites, Part B 43 (2012) 1943–1954.

[11] Z.X. Lei, L.W. Zhang, K.M. Liew, Buckling analysis of CNT reinforced functionally graded laminated composite plates, Compos. Struct. 152 (2016) 62–73.

[12] H.S. Shen, Y. Xiang, Nonlinear bending of nanotube-reinforced composite cylindrical panels resting on elastic foundations in thermal environments, Eng. Struct. 80 (2014) 163–172.

[13] H.S. Shen, Y. Xiang, Nonlinear vibration of nanotube-reinforced composite cylindrical panels resting on elastic foundations in thermal environments, Compos. Struct. 111 (2014) 291–300.

[14] M. Mirzaei, Y. Kiani, Thermal buckling of temperature dependent FG-CNT reinforced composite plates, Meccanica 47 (2015) 1–17.

[15] R. Kolahchi, M. Safari, M. Esmailpour, Dynamic stability analysis of temperature-dependent functionally graded CNT-reinforced visco-plates resting on orthotropic elastomeric medium, Compos. Struct. 150 (2016) 255–265.

[16] L.W. Zhang, W.H. Liu, K.M. Liew, Geometrically nonlinear large deformation analysis of triangular CNT-reinforced composite plates, Int. J. Non-Linear Mech. 86 (2016) 122–132.

[17] H. Zhu, S.K. Khanna, Dynamic response of a novel laminated glass panel using a transparent glass fiber-reinforced composite interlayer under blast loading, Int. J. Impact Eng. 89 (2016) 14–24.

[18] C. Ding, T. Ngo, P. Mendis, R. Lumantarna, M. Zobec, Dynamic response of double skin façades under blast loads, Eng. Struct. 123 (2016) 155–165.

[19] P. Zhang, Y. Cheng, J. Liu, C. Wang, H. Hou, Y. Li, Experimental and numerical investigations on laser-welded corrugated-core sandwich panels subjected to air blast loading, Mar. Struct. 40 (2015) 225–246.

[20] E.A. Flores-Johnson, L. Shen, I. Guiamatsia, G.D. Nguyen, A numerical study of bioinspired nacre-like composite plates under blast loading, Compos. Struct. 126 (2015) 329–336.

[21] N. Lam, P. Mendis, Ngo T. Response, Spectrum solutions for blast loading, Electron. J. Struct. Eng. 4 (2004) 28–44.

[22] K. Micallef, A.S. Fallah, D.J. Pope, L.A. Louca, The dynamic performance of simply-supported rigid-plastic circular steel plates subjected to localised blast loading, Int. J. Mech. Sci. 65 (2012) 177–191.

[23] S. Yao, D. Zhang, X. Chen, F. Lu, W. Wang, Experimental and numerical study on the dynamic response of RC slabs under blast loading, Eng. Fail. Anal. 66 (2016) 120–129.

[24] A. Arablouei, V. Kodur, Modeling delamination of fire insulation from steel structures subjected to blast loading, Eng. Struct. 116 (2016) 56–69.

[25] N.D. Duc, N.D. Tuan, P. Tran, T.Q. Quan, Nonlinear dynamic response and vibration of imperfect shear deformable functionally graded plates subjected to blast and thermal loads, Mech. Adv. Mat. Struct. 24 (2017) 318–329.

[26] V. Pickerd, H. Bornstein, P. McCarthy, M. Buckland, Analysis of the structural response and failure of containers subjected to internal blast loading, Int. J. Impact Eng. 95 (2016) 40–53.

[27] P. Tran, T.D. Ngo, A. Ghazlan, Numerical modelling of hybrid elastomeric composite panels subjected to blast loadings, Compos. Struct. 153 (2016) 108–122.

[28] P. Del Linz, X. Liang, P.A. Hooper, L.Z. Wang, J.P. Dear, An analytical solution for pre-crack behaviour of laminated glass under blast loading, Compos. Struct. 144 (2016) 156–164.
[29] I. Eshraghi, S. Dag, N. Soltani, Bending and free vibrations of functionally graded annular and circular micro-plates under thermal loading, Compos. Struct. 137 (2016) 196–207.
[30] N.D. Duc, Nonlinear thermal dynamic analysis of eccentrically stiffened S-FGM circular cylindrical shells surrounded on elastic foundations using the Reddy's third-order shear deformation shell theory, Eur. J. Mech. A, Solids 58 (2016) 10–30.
[31] M. Mirsalehi, M. Azhari, H. Amoushahi, Stability of thin FGM microplate subjected to mechanical and thermal loading based on the modified couple stress theory and spline finite strip method, Aerosp. Sci. Technol. 47 (2015) 356–366.
[32] J. Sun, C.W. Lim, X. Xu, H. Mao, Accurate buckling solutions of grid-stiffened functionally graded cylindrical shells under compressive and thermal loads, Composites Part B, Engineering 89 (2016) 96–107.
[33] D.H. Bich, N.D. Duc, T.Q. Quan, Nonlinear vibration of imperfect eccentrically stiffened functionally graded double curved shallow shells resting on elastic foundation using the first order shear deformation theory, Int. J. Mech. Sci. 80 (2014) 16–28.
[34] F. Guo, K. Huang, L. Guo, X. Bai, S. Zhong, H. Yu, An interaction energy integral method for T-stress evaluation in nonhomogeneous materials under thermal loading, Mech. Mater. 83 (2015) 30–39.
[35] A. Warminska, E. Manoach, J. Warminski, Vibrations of a composite beam under thermal and mechanical loadings, Proc. Eng. 144 (2016) 959–966.
[36] N.S. Bardell, D.J. Mead, Free vibration of an orthotropic stiffened cylindrical shell. Part I: discrete line simple supports, J. Sound Vib. 134 (1989) 29–54.
[37] Y-C. Chern, C.C. Chao, Comparison of natural frequencies of laminates by 3-D theory. Part II: curved panels, J. Sound Vib. 230 (2000) 1009–1030.
[38] H. Matsunaga, Free vibration and stability of functionally graded shallow shells according to a 2-D higher-order deformation theory, Compos. Struct. 84 (2008) 132–146.
[39] N.D. Duc, Nonlinear dynamic response of imperfect eccentrically stiffened FGM double curved shallow shells on elastic foundation, Compos. Struct. 102 (2012) 306–314.
[40] N.D. Duc, T.Q. Quan, V.D. Luat, Nonlinear dynamic analysis and vibration of shear deformable piezoelectric FGM double curved shallow shells under damping-thermo-electro-mechanical loads, Compos. Struct. 125 (2015) 29–40.
[41] T.Q. Quan, Phuong Tran, N.D. Tuan, N.D. Duc, Nonlinear dynamic analysis and vibration of shear deformable eccentrically stiffened S-FGM cylindrical panels with metal-ceramic-metal layers resting on elastic foundations, Compos. Struct. 126 (2015) 16–33.
[42] N.D. Duc, Nonlinear Static and Dynamic Stability of Functionally Graded Plates and Shells, Vietnam National University Press, Hanoi, Vietnam, 2014.
[43] D.D. Brush, B.O. Almroth, Buckling of Bars, Plates and Shells, McGraw-Hill, 1975.
[44] J.N. Reddy, Mechanics of Laminated Composite Plates and Shells: Theory and Analysis, CRC Press, Boca Raton, 2004.